

Learning from higher-order statistics, efficiently: hypothesis tests, random features, and neural networks

Eszter Székely*, Lorenzo Bardone*, Federica Gerace and Sebastian Goldt†

International School of Advanced Studies (SISSA), Trieste, Italy

20th February 2024

Abstract

Neural networks excel at discovering statistical patterns in high-dimensional data sets. In practice, higher-order cumulants, which quantify the non-Gaussian correlations between three or more variables, are particularly important for the performance of neural networks. But how efficient are neural networks at extracting features from higher-order cumulants? We study this question in the spiked cumulant model, where the statistician needs to recover a privileged direction or “spike” from the order- $p \geq 4$ cumulants of d -dimensional inputs. We first characterise the fundamental statistical and computational limits of recovering the spike by analysing the number of samples n required to strongly distinguish between inputs from the spiked cumulant model and isotropic Gaussian inputs. We find that statistical distinguishability requires $n \gtrsim d$ samples, while distinguishing the two distributions in polynomial time requires $n \gtrsim d^2$ samples for a wide class of algorithms, i.e. those covered by the low-degree conjecture. These results suggest the existence of a wide statistical-to-computational gap in this problem. Numerical experiments show that neural networks learn to distinguish the two distributions with quadratic sample complexity, while “lazy” methods like random features are not better than random guessing in this regime. Our results show that neural networks extract information from higher-order correlations in the spiked cumulant model efficiently, and reveal a large gap in the amount of data required by neural networks and random features to learn from higher-order cumulants.

1 Introduction

Discovering statistical patterns in high-dimensional data sets is the key objective of machine learning. In a classification task, the differences between inputs in different classes arise at different statistical levels of the inputs: two different classes of images will usually have different means, different covariances, and different higher-order cumulants (HOCs), which describe the non-Gaussian part of the correlations between three or more pixels. While differences in the mean and covariance allow for rudimentary classification, Refinetti *et al.* [1] recently highlighted the importance of HOCs for the performance of neural networks: when they removed the HOCs per class of the CIFAR10 training set, the test accuracy of various deep neural networks dropped by up to 65 percentage points. The importance of higher-order cumulants (HOCs) for classification in general and the performance of neural networks in particular raises some fundamental questions: what are the fundamental limits of learning from HOCs, i.e. how many samples n (“sample complexity”) are required to extract information from the HOCs of a data set? How many samples are required when using a *tractable* algorithm? And how do neural networks and other machine learning methods like random features compare to those fundamental limits?

In this paper, we study these questions by analysing a series of binary classification tasks. In one class, inputs $x \in \mathbb{R}^d$ are drawn from a normal distribution with zero mean and identity covariance.

*These authors contributed equally

†{eszekely, lbardone, fgerace, sgoldt}@sisssa.it

These inputs are therefore isotropic: the distribution of the high-dimensional points projected along a unit vector in any direction in \mathbb{R}^d is a standard Gaussian distribution. Furthermore, all the higher-order cumulants (of order $p \geq 3$) of the inputs are identically zero. Inputs in the second class are also isotropic, except for one special direction $u \in \mathbb{R}^d$ in which their distribution is different. This direction u is often called a “spike”, and it can be encoded in different cumulants: for example, we could “spike” the covariance by drawing inputs from a Gaussian with mean zero and covariance $\mathbb{I} + \beta uu^\top$; the signal-to-noise ratio $\beta > 0$ would then control the variance of $\lambda = \langle u, x \rangle$. Likewise, we could spike a higher-order cumulant of the distribution and ask: what is the minimal number of samples required for a neural network trained with SGD to distinguish between the two input classes? This simple task serves as a proxy for more generic tasks: a neural network will not be able to *extract* information from a given cumulant if it cannot even recognise that it is different from an isotropic one (in all the cases we will study, detecting an anisotropy in the distribution and recovering the spike require the same number of samples, a notion we will make more precise in section 2.1).

We can obtain the fundamental limits of detecting spikes at different levels of the cumulant hierarchy by considering the hypothesis test between a null hypothesis (the isotropic multivariate normal distribution with zero mean and identity covariance) and an alternative “spiked” distribution. We can then compare the sample complexity of neural networks to the number of samples necessary to distinguish the two distributions using unlimited computational power, or efficiently using algorithms that run in polynomial time. A second natural comparison for neural networks are random features or kernel methods. Since the discovery of the neural tangent kernel [2], and the practical success of kernels derived from neural networks [3, 4], there has been intense interest in establishing the advantage of neural networks with *learned* feature maps over classical methods with *fixed* feature maps, like kernel machines. The role of higher-order correlations for the relative advantage of these methods has not been studied yet.

In the following, we first introduce some fundamental notions around hypothesis tests and in particular the low-degree method [5–8], which will be a key tool in our analysis, using the classic spiked Wishart model for sample covariance matrices [9, 10] (section 2). Our **main contributions** are then as follows:

- We investigate the sample complexity of learning from HOCs using unbounded computational power. An analysis of the *likelihood ratio* norm reveals that a number of samples *linear* in the input dimension is sufficient to pass the *second moment method for distinguishability* (3.2).
- With bounded computational power, we show that the sample complexity of learning from HOCs is instead *quadratic* for a wide class of polynomial-time algorithms (section 3.3), suggesting the existence of a wide *computational-to-statistical gap* in this model.
- We use these fundamental limits on learning from HOCs to show numerically that neural networks learn the mixed cumulant model efficiently, while random features do not, revealing a large separation between the two methods (sections 4.1 and 4.2).
- We finally show numerically that the distinguishability in a simple model for images [11] is precipitated by a cross-over in the behaviour of the higher-order cumulants of the inputs (section 4.3).

Further related work

Detecting spikes in high-dimensional data There is an enormous literature on statistical-to-computational gaps in the detection and estimation of variously structured principal components of high-dimensional data sets. This problem has been studied for the Wigner and Wishart ensembles of random matrices [9, 12–22] and for spiked tensors [23–31]. For comprehensive reviews of the topic, see refs. [32–35]. While the samples in these models are often non-Gaussian, depending on the prior distribution over the spike u , the spike appears already at the level of the covariance of the inputs. Here, we instead study a high-dimensional data model akin to the one used by Wang & Lu [36] to study online

independent component analysis (ICA). This data model can be interpreted as having an additional whitening step to pre-process the inputs, which is a common pre-processing step in ICA [37], hence inputs have identity covariance even when cumulants of order $p \geq 3$ are spiked. Wang & Lu [36] proved the existence of a scaling limit for online ICA, but did not consider the sample complexity of recovering the spike, which is the focus of this paper for a wide class of algorithms.

Separation between neural networks and random features The discovery of the neural tangent kernel by Jacot *et al.* [2], and more generally the flurry of results on linearised neural networks [2, 3, 38–44], has triggered a new wave of interest in the differences between what neural networks and kernel methods can learn efficiently. While statistical separation results have been well-known for a long time [45], recent work focused on understanding the differences between random features and neural networks *trained by gradient descent* both with wide [4, 46–50] or even with just a few hidden neurons [51, 52]. At the heart of the data models in all of these theoretical models is a hidden, low-dimensional structure in the task, either in input space (for mixture classification) or in the form of single- or many-index target functions. The impact of higher-order input correlations in mixture classification tasks on the separation between random features and neural networks has not been studied directly yet.

Reproducibility

We provide code for all of our experiments, including routines to generate the various synthetic data sets we discuss, on GitHub <https://github.com/eszter137/data-driven-separation>.

2 Warm-up: the Gaussian case

We set the scene by considering a Gaussian model for data first. This simple setup allows us to introduce the machinery necessary to analyse the spiked cumulant model that we present in section 3. We consider high-dimensional inputs $x^\mu = (x_i^\mu) \in \mathbb{R}^d$ with label $y^\mu = \pm 1$ for the two classes. The total number of training samples is $2n$, i.e. we have n samples per class. For the class $y^\mu = -1$, inputs $x^\mu = z^\mu$, where $z^\mu \sim_{\text{iid}} \mathcal{N}(0, \mathbb{1}_d)$ and \mathcal{N} denotes the normal distribution. For the class $y^\mu = 1$ instead, we generate inputs as

$$x^\mu = \sqrt{\frac{\beta}{d}} g^\mu u + z^\mu, \quad g^\mu \sim_{\text{iid}} \mathcal{N}(0, 1), \quad (1)$$

where $u = (u_i)$ is a d -dimensional vector with norm $\|u\| = \sqrt{d}$ whose elements are drawn element-wise i.i.d. according to some probability distribution \mathcal{P}_u . Equation (1) is of course the well-known spiked Wishart model from random matrix theory [9, 10], where inputs are isotropic except in the direction of the “spike” u , where they have variance $1 + \beta$ with the signal-to-noise ratio $\beta > 0$. It can be easily verified that the inputs in the second class are normally distributed with mean 0 and covariance $\Sigma = \mathbb{1} + \beta/d uu^\top$. We refer to the class $y^\mu = 1$ as the spiked class.

2.1 When can the two classes be distinguished, efficiently?

The classification problem of distinguishing isotropic Gaussian inputs from the spiked Wishart model can equivalently be seen as a hypothesis test: how many samples does a statistician need to determine whether a data set comes from the null model $\mathcal{N}(0, \mathbb{1}_d)$ or the spiked model $\mathcal{N}(0, \mathbb{1}_d + \beta/d uu^\top)$? We are interested in the problem of distinguishing the two statistical models in two scenarios: with unbounded and bounded computational resources.

2.1.1 Statistical and computational distinguishability

From a statistical point of view, distinguishing two sequences of probability measures $\mathbb{P} = (\mathbb{P}_n)_{n \in \mathbb{N}}$ and $\mathbb{Q} = (\mathbb{Q}_n)_{n \in \mathbb{N}}$ defined on a sequence of measure spaces $(\Omega_n, \mathcal{F}_n)$ means finding a sequence of tests $f_n : \Omega_n \rightarrow \{0, 1\}$, which are measurable functions that indicate whether a given set of inputs

was sampled from \mathbb{P} or \mathbb{Q} . We will say that the two measures are **statistically distinguishable** in the strong sense if there exists a statistical test f for which

$$\mathbb{Q}_n(f_n(x) = 0) \xrightarrow{n \rightarrow \infty} 1 \quad \text{and} \quad \mathbb{P}_n(f_n(x) = 1) \xrightarrow{n \rightarrow \infty} 1. \quad (2)$$

The strong version of statistical distinguishability requires that the probability of success of the statistical test must tend to 1 as $n \rightarrow \infty$, whereas **weak distinguishability** just requires it to be asymptotically greater than $1/2 + \varepsilon$, for any $\varepsilon > 0$. We will call the minimal number of samples required to achieve strong statistical distinguishability the **statistical sample complexity** of the problem. We can obtain a computationally bounded analogue of this definition by restricting the complexity of the statistical test f_n to functions that are computable in a time that is polynomial in the input dimension d . The **computational statistical complexity** is then the minimal number of samples required to achieve **computational distinguishability**.

2.1.2 Necessary conditions for distinguishability

A necessary condition for strong distinguishability is based on the *likelihood ratio* (LR) of probability measures, which is defined as

$$L_n(x) := \frac{d\mathbb{P}_n}{d\mathbb{Q}_n}(x) \quad (3)$$

The likelihood ratio provides a necessary condition for strong distinguishability of \mathbb{P} and \mathbb{Q} via the so-called second moment method:

Proposition 2.1 (Second Moment Method for Distinguishability). *Suppose that \mathbb{P}_n is absolutely continuous with respect to \mathbb{Q}_n , and let L_n be the corresponding LR. A necessary condition for strong distinguishability of \mathbb{P} from \mathbb{Q} is*

$$\|L_n\|^2 := \mathbb{E}_{x \sim \mathbb{Q}_n} [L_n(x)^2] \xrightarrow{n \rightarrow \infty} +\infty. \quad (4)$$

where $\|\cdot\|$ is the norm with respect to the Hilbert space

$$L^2(\Omega_n, \mathbb{Q}_n) = \{f : \Omega_n \rightarrow \mathbb{R} \mid \mathbb{E}_{\mathbb{Q}_n}[f^2(x)] < \infty\}. \quad (5)$$

The second moment method has been used to derive statistical thresholds for various high-dimensional inference problems [17, 25, 35, 53]. Note that proposition 2.1 only states a necessary condition; while it is possible to construct counterexamples, they are usually based on rather artificial constructions [35], and the second moment method is considered a good proxy for strong statistical distinguishability.

However, proposition 2.1 does not tell us anything about the required number of samples to distinguish the two distributions *efficiently*, i.e. by using an algorithm that only requires a time that is polynomial in the input dimension. The algorithmic sample complexity required to distinguish the two classes efficiently can be analysed rigorously for a wide class of algorithms using the *low-degree method* [5–8, 35]. The low-degree method arose from the study of the sum-of-squares hierarchy [5] and rose to prominence when Hopkins & Steurer [7] demonstrated that the method can capture the Kesten-Stigum threshold for community detection in the stochastic block model [54–56]. In the case of hypothesis testing, the key quantity is the *low-degree likelihood ratio* (LDLR) [8, 35].

Definition 2.2 (Low-degree likelihood ratio (LDLR)). Let $D \geq 0$ be an integer. The low-degree likelihood ratio of degree D is defined as

$$L^{\leq D} := \mathcal{P}^{\leq D} L \quad (6)$$

where $\mathcal{P}^{\leq D}$ projects L onto the space of polynomials of degree up to D , parallel to the Hilbert space structure defined by the scalar product $\langle f, g \rangle_{L^2(\Omega, \mathbb{Q})} := \mathbb{E}_{x \sim \mathbb{Q}}[f(x)g(x)]$.

The idea of this method is that among degree- D polynomials, $L^{\leq D}$ captures optimally the difference between \mathbb{P} and \mathbb{Q} , and this difference can be quantified by the norm $\|L^{\leq D}\| = \|L^{\leq D}\|_{L^2(\Omega_n, \mathbb{Q}_n)}$. Hence in analogy to proposition 2.1, we can expect low-degree polynomials to be able to distinguish \mathbb{P} from \mathbb{Q} only when $\|L_n^{\leq D(n)}\| \xrightarrow{n} \infty$, where $D(n)$ is a monotone sequence diverging with n . Indeed, the following (informal) conjecture from Hopkins [8] states that this criterion is valid not only for polynomial tests, but for all polynomial-time algorithms:

Conjecture 2.3. For two sequences of measures $\mathbb{Q}_N, \mathbb{P}_N$ indexed by N , suppose that (i) \mathbb{Q}_N is a product measure; (ii) \mathbb{P}_N is *sufficiently* symmetric with respect to permutations of its coordinates; and (iii) \mathbb{P}_N is *robust* with respect to perturbations with small amount of random noise. If $\|L_N^{\leq D}\| = O(1)$ as $N \rightarrow \infty$ and for $D \geq (\log N)^{1+\varepsilon}$, for some $\varepsilon > 0$, then there is no polynomial-time algorithm that strongly distinguishes the distributions \mathbb{Q} and \mathbb{P} .

Even though this conjecture is still not proved in general, its empirical confirmation on many benchmark problems has made it an important tool to probe questions of computational complexity, see Kunisky *et al.* [35] for an overview. For instance, in the present case of the spiked Wishart model, the LDLR method correctly finds both the right scaling of d, n and the critical value for the signal-to-noise ratio to distinguish the two distributions, as was shown by Bandeira *et al.* [57] for a more general model that encompasses the spiked Wishart. Here, we give a simple and more direct LDLR analysis of the spiked Wishart model which will be the starting point of our analysis of the spiked cumulant model:

Theorem 2.4 (LDLR for spiked Wishart model). *Suppose the prior on u belongs to the following cases:*

- $(u_i)_{i=1,\dots,d}$ are i.i.d. and symmetric Rademacher random variables
- $(u_i)_{i=1,\dots,d}$ are i.i.d. and $u_i \sim \mathcal{N}(0, 1)$

Let $D \in \mathbb{N}$ and $d, n \rightarrow \infty$, with fixed ratio $\gamma := d/n$, then

$$\lim_{d, n \rightarrow \infty} \|L^{\leq D}\| = \sum_{k=0}^D \frac{(2k-1)!!}{(2k)!!} \frac{\beta^{2k}}{\gamma^k}, \quad (7)$$

which, as D increases, stays bounded for $\beta < \beta_c := \sqrt{\gamma} = \sqrt{d/n}$ and diverges for $\beta > \beta_c$.

The distinguishability threshold that we have recovered here is of course the famous BBP phase transition in the spiked Wishart model [9]: if $\beta < \beta_c = \sqrt{d/n}$, the low-degree likelihood ratio stays bounded and indeed a set of inputs drawn from eq. (1) is statistically indistinguishable from a set of inputs drawn from $\mathcal{N}(0, \mathbb{I})$. For $\beta > \beta_c$ instead, there is a phase transition for the largest eigenvalue of the empirical covariance of the inputs in the second class, which can be used to differentiate the two classes, and the LDLR diverges. The proof of theorem 2.4 follows from a straightforward application of the LDLR analysis of *additive Gaussian models* [35], see appendix B.2.1. Note that for the spiked Wishart model, we obtain the correct BBP threshold for the signal-to-noise ratio via theorem 2.4 even when we restrict ourselves to the class of polynomials of constant degree. For the analysis of the spiked cumulant model that we consider next, we will consider polynomials of diverging degree as per the low-degree conjecture 2.3.

3 Beyond Gaussianity: efficient learning from higher-order cumulants

3.1 The spiked cumulant model

In the Wishart model, inputs in both classes are Gaussian, so all higher-order cumulants of the inputs are identically 0. To study specifically the impact of HOCs, we study the data model used by Wang & Lu [36] to study online independent component analysis (ICA). We will refer to this model as *spiked cumulant model* to emphasise the analogy to the spiked Wishart model. For the class $y^\mu = -1$, inputs

remain element-wise i.i.d. Gaussian random vectors in d dimensions as before, $x^\mu = z^\mu$. For the “spiked” class $y^\mu = 1$, we draw inputs in two steps. First, we sample inputs \tilde{x}^μ similarly to the spiked Wishart model, except that we change the distribution of the scalar latent variables g^μ to some non-Gaussian distribution $p_g(g^\mu)$

$$\tilde{x}^\mu = \sqrt{\frac{\beta}{d}} g^\mu u + z^\mu, \quad g^\mu \sim_{\text{i.i.d.}} p_g. \quad (8)$$

We could for example draw g^μ from the Rademacher distribution; see assumption 3.1 for a precise statement. For any non-Gaussian p_g , the resulting inputs x^μ will not be normally distributed anymore; instead, their fourth-order cumulant is given by $\kappa_{i,j,k,l} \equiv \mathbb{E} x_i x_j x_k x_l - \mathbb{E} x_i x_j \mathbb{E} x_k x_l [3] = \frac{\beta^2}{d^2} \kappa_4^g u_i u_j u_k u_l$, where the brackets $[3]$ denote the three permutations over the indices in the second term, and $\kappa_4^g \equiv \mathbb{E} (g^\mu)^4 - 3\mathbb{E} (g^\mu)^2$ is the fourth cumulant of the distribution of g^μ . Note that all higher-order cumulants are spiked. We fix the mean and variance of p_g to be zero and one, respectively, so the covariance of inputs drawn from eq. (8) has the same covariance matrix as the inputs in the spiked Wishart model, $\Sigma = \mathbb{1}_d + \beta/d u u^\top$. To avoid trivial detection of the non-Gaussianity by looking at the covariance of inputs, the key ingredient of the spiked cumulant model is that we whiten the inputs in that class, so that the inputs are finally given by

$$x^\mu = S \tilde{x}^\mu, \quad S = \mathbb{1} - \frac{\beta}{1 + \beta + \sqrt{1 + \beta}} \frac{u u^\top}{d}, \quad (9)$$

with the whitening matrix S (see appendix B.3.3). Hence inputs x^μ are isotropic Gaussians in all directions except u , where they are a weighted sum of g^μ and $\langle z, u \rangle$. The whitening therefore changes the interpretation of β : rather than being a signal-to-noise ratio, as in the spiked Wishart model, here β controls the quadratic interpolation between the distributions of g^μ and z in the direction of u , see appendix B.3.3.

This leaves us with a data set where inputs in both classes have an average covariance matrix that is the identity, which means that PCA or linear neural networks [58–61] cannot detect any difference between the two classes. Given a data set sampled from the spiked cumulant model, we can now ask: how many samples does a statistician need to reliably detect whether inputs are Gaussian or not, i.e. whether HOCs are spiked or not? This is equivalent to the hypothesis test between the isotropic normal distribution as the null hypothesis \mathbb{Q} , and the spiked cumulant model eq. (9) as the alternative hypothesis \mathbb{P} . It is not possible to analyse this hypothesis test using results for additive Gaussian noise models: the whitening step destroys the additive noise structure because the matrix S applies a non rotationally-invariant transformation that depends on the unknown spike u ; instead, we have to develop new tools to analyze the hypothesis test.

3.2 Statistical distinguishability: LR analysis

We first focus on the question of detecting non-Gaussianity in a data matrix $\underline{x} = (x^\mu)_{1,\dots,n}^\top$ using unlimited computational resources. Here and throughout, we will denote matrices of size $n \times d$ with underlined letters; see appendix B.1.1 for a complete summary of our notation. We will use Hermite polynomials, denoted by $(h_k)_k$, see appendix B.1.2 for details. We assume that the spike u is drawn from a known prior $\mathcal{P}(u)$, and that the scalar latent variables $(g^\mu)_{\mu=1,\dots,n}$ are drawn i.i.d. from a distribution p_g with the following properties:

Assumption 3.1 (Assumption on latent variables g^μ). We assume that the one-dimensional probability distribution of the non-Gaussian random variable $p_g(g)$ is an even distribution, $p_g(g = dx) = p_g(-g = -dx)$, with mean 0 and variance 1, and that it satisfies the following requirement on the growth of its Hermite coefficients:

$$\mathbb{E} [h_m(g)] \leq \Lambda^m m! \quad (10)$$

where $\Lambda > 0$ is a positive constant that does not depend on m . Finally, we assume that p_g has tails that cannot go to 0 slower than a standard Gaussian, $\mathbb{E}[\exp(g^2/2)] < +\infty$.

A detailed discussion of these assumptions, as well as proof that they are satisfied by a wide class of distributions (including Rademacher(1/2) and Unif($-\sqrt{3}, \sqrt{3}$)) can be found in appendix B.3. Focusing on the high-dimensional regime where $n, d \rightarrow \infty$ with $n \asymp d^\theta$, where $\theta > 0$ is the *sample complexity exponent*, we want to determine the smallest value of θ for which it is possible to achieve strong distinguishability between Gaussian and non-Gaussian data. Following the second moment method for distinguishability, proposition 2.1, we need to compute the norm of the likelihood ratio, which we characterise in the following theorem:

Theorem 3.2. *Suppose that u has i.i.d. Rademacher prior and that the non-Gaussian distribution p_g satisfies assumption 3.1. Then the norm of the total LR is given by*

$$\|L_{n,d}\|^2 = \sum_{j=0}^d \binom{d}{j} \frac{1}{2^d} f\left(\beta, \frac{2j}{d} - 1\right)^n, \quad (11)$$

where $f(\beta, \lambda)$ is a scalar function of order $O(1)$ given by a two-dimensional average over the non-Gaussian distribution p_g , eq. (B.48).

We sketch the proof of the theorem in appendix B.4.1 whereas the complete details can be found in appendix B.4. The key consequence of theorem 3.2 is that taking $g \sim \text{Rademacher}(1/2)$, we have $\max_\lambda f(\beta, \lambda) = f(\beta, 1) > 1$, so using eq. (11) we find that

$$\|L_{n,d}\| \geq \frac{f(\beta, 1)^n}{2^d}. \quad (12)$$

For Rademacher prior on g , the LR norm thus diverges as soon as n grows as $n \asymp d^\theta$ with $\theta > 1$. As detailed in appendix B.4.3, $\|L_{n,d}\|$ even diverges for $\theta = 1$ and $d \asymp \gamma n$ for some $\gamma > 0$, which is the same sample complexity as in the spiked Wishart model, theorem 2.4. Note that theorem 3.2 does not imply that the likelihood ratio is bounded at any sample complexity, however computing explicitly LR norm using eq. (11) (see fig. B.2) confirms the intuition that the LR norm is bounded for $\theta < 1$. The linear sample complexity for the statistical threshold of detecting non-Gaussianity is also consistent with the statistical threshold for tensor PCA [30]. We will now compare this statistical threshold with the *computational sample complexity exponent* that quantifies the sample complexity of detecting non-Gaussianity with an efficient algorithm.

3.3 Computational distinguishability: LDLR analysis

We now turn to the *computational sample complexity exponent* that quantifies the sample complexity of detecting non-Gaussianity with an efficient algorithm. Keeping the notation of section 3.2, we consider the same high-dimensional regime $n, d \rightarrow \infty$ with $n \asymp d^\theta$. This time, we want to determine the smallest value of θ for which it is possible to achieve strong distinguishability *in polynomial time*. The criterion for computationally efficient distinguishability is the divergence of the low-degree likelihood ratio (LDLR), so we first characterise the behaviour of the LDLR by proving the following upper and lower bounds:

Theorem 3.3 (LDLR for spiked cumulant model). *Suppose that $(u_i)_{i=1,\dots,d}$ are drawn i.i.d. from the symmetric Rademacher distribution. If the non-Gaussian distribution p_g satisfies assumption 3.1, then the following lower and upper bounds hold:*

- Let $D \in \mathbb{N}$ such that $D/4 \leq n$, then:

$$\|L_{n,d}^{\leq D}\|^2 \geq \sum_{m=0}^{\lfloor D/4 \rfloor} \binom{n}{m} \binom{d+1}{2}^m \left(\frac{\beta^2 \kappa_4^g}{\sqrt{4!} d^2 (1 + \beta)^2} \right)^{2m}. \quad (13)$$

where κ_4^g is the fourth order cumulant of g .

- Conversely, for any D, n, d :

$$\left\| L_{n,d}^{\leq D} \right\|^2 \leq 1 + \sum_{m=1}^D \frac{C_m}{d^m} \sup_{k \leq m} \left(\mathbb{E} [h_k(g)]^{2m/k} \right) \binom{n}{\lfloor m/4 \rfloor} \binom{d}{\lfloor m/2 \rfloor} \quad (14)$$

$$\text{where } C_m := \left(\frac{\beta}{1+\beta} \right)^m \binom{\lfloor m/4 \rfloor \lfloor m/2 \rfloor + m - 1}{m}.$$

We sketch the proof of theorem 3.3 in appendix B.5.1 and give the complete proof in appendix B.5.2. The bounds of theorem 3.3 hold for any n, d (requiring $D/4 \leq n$ just for the lower bound). The sample complexity in the high-dimensional regime $n, d \rightarrow \infty$ with $n \asymp d^\theta$ can be derived from the asymptotic behaviour of the bounds which we establish in the following corollary:

Corollary 3.4 (Asymptotics of LDLR bounds). *Assume the hypotheses of theorem 3.3. Let $0 < \varepsilon < 1$ and assume $D(n) \asymp \log^{1+\varepsilon}(n)$. Take $n, d \rightarrow \infty$, with the scaling $n \asymp d^\theta$ for $\theta > 0$. Estimate eq. (13) implies that for n, d large enough, the following lower bound holds:*

$$\left\| L_{n,d}^{\leq D(n)} \right\|^2 \geq \left(\frac{1}{\lfloor D(n)/4 \rfloor} \left(\frac{\beta^2 \kappa_4^g}{(1+\beta)^2} \right)^2 \frac{n}{d^2} \right)^{\lfloor D(n)/4 \rfloor} \quad (15)$$

Conversely, eq. (14) leads to:

$$\left\| L_{n,d}^{\leq D(n)} \right\|^2 \leq 1 + \sum_{m=1}^{D(n)} \left(\frac{\Lambda^2 \beta}{1+\beta} \right)^m m^{4m} \left(\frac{n}{d^2} \right)^{m/4} \quad (16)$$

Taken together, eqs. (15) and (16) imply the presence of a critical regime for $\theta_c = 2$, and describe the behaviour of $\left\| L_{n,d}^{\leq D} \right\|^2$ for all $\theta \neq \theta_c$

$$\lim_{n,d \rightarrow \infty} \left\| L_{n,d}^{\leq D(n)} \right\|^2 = \begin{cases} 1 & 0 < \theta < 2 \\ +\infty & \theta > 2 \end{cases} \quad (17)$$

We prove corollary 3.4 using standard asymptotic approximations to isolate the terms depending on n and d in eq. (13) and eq. (14), see appendix B.5.2 for the rigorous argument. If we assume the low-degree conjecture 2.3, theorem 3.3 and corollary 3.4 give a complete picture of the sample complexity for efficient detection of non-Gaussianity:

- For a number of samples $n \asymp d^\theta$ with sample complexity exponent $\theta < 2$, no polynomial-time algorithm is able to strongly distinguish the spiked cumulant distribution from white noise.
- If instead $\theta > 2$, then distinguishability in polynomial time is possible (fig. B.2). Moreover, the proofs indicate that order-4 polynomial tests are able to achieve it.

At the transition point $\theta = 2$, the leading terms of eqs. (15) and (16) disappear, and terms like D^{-D} for the lower bound and D^D for upper bound dominate, so the bounds do not match anymore, making it impossible to deduce the behaviour of the LDLR. Those terms are likely artefacts of the proof method, and a finer analysis could be able to improve the bounds to obtain sharper dependencies on β and the cumulants of g at the critical regime $\theta = 2$.

3.4 Statistical-to-computational gaps in the spiked cumulant model

Put together, our results for the statistical and computational sample complexities of detecting non-Gaussianity in theorem 3.2 and corollary 3.4 suggest the existence of three different regimes in the spiked cumulant model as we vary the exponent θ , with a statistical-to-computational gap:

- For $0 \leq \theta < 1$, the problem appears *statistically impossible* in the sense that no algorithm should be able to strongly distinguish \mathbb{P} and \mathbb{Q} with so few samples.
- For $1 < \theta < 2$, the norm of the likelihood ratio with $g \sim \text{Rademacher}(1/2)$ diverges (even at $\theta = 1$ for some values of β), the problem is statistically solvable, yet no polynomial-time algorithm is known; this is the so-called *hard phase*.
- If $\theta > 2$ the problem is solvable in polynomial time by evaluating a polynomial function and thresholding; this is the *easy phase*.

Hypothesis testing for the spiked cumulant model is thus an intrinsically harder problem than classification for spiked Wishart model, where the critical regime is at linear sample complexity. The proof of theorem 3.3 reveals that this increased difficulty is a direct consequence of the whitening of the inputs, eq. (9). Without whitening, degree-2 polynomials would also give contributions to the LDLR (B.51) which would yield linear sample complexity. The difference in sample complexity of the spiked Wishart and spiked cumulant models mirrors the gap between the sample complexity of the best-known algorithms for matrix factorisation, which require linear sample complexity, and tensor PCA for rank-1 spiked tensors of order k [23, 26, 28], where sophisticated spectral algorithms can match the computational lower bound of $d^{k/2}$ samples.

As is generally the case in high-dimensional statistics, our results do not constitute a complete proof of the existence of a statistical to computational gap: our argument relies on the low-degree conjecture 2.3, and the divergence of the norm of the likelihood ratio is only a necessary condition for *strong distinguishability*. In fact, there are no techniques at the moment that can prove that average-case problems require super-polynomial time in the hard phase, even assuming $P \neq NP$ [35], so our work should be seen as providing rigorous evidence for a statistical-to-computational gap in the spike cumulant model. We finally note that as soon as the sample complexity exponent is greater than 2, strong distinguishability is possible even when we ignore all the information in cumulants with order higher than 4. This implies that order-4 polynomial tests can be used to solve the hypothesis testing problem in this regime.

4 Learning from HOCs with neural networks and random features

The analysis of the (low-degree) likelihood ratio has given us a detailed picture of the statistical and computational complexity of learning from the covariance or the higher-order cumulants of data. We will now use these fundamental limits to benchmark the sample complexity of some specific algorithms: neural networks trained with stochastic gradient descent, and random features [62–64], which are a finite-dimensional approximation of kernel methods. We will see that the spiked cumulant model exhibits a large gap in the sample complexity required for neural networks or random features. We give full details on the experiments in appendix A.

4.1 Spiked Wishart model

We trained two-layer ReLU neural networks $\phi_\theta(x) = v^\top \max(0, w^T x)$ with $m = 5d$ hidden neurons on the spiked Wishart classification task. We show the early-stopping test accuracy of the networks in the linear and quadratic regimes with $n_{\text{class}} \asymp d, d^2$ samples per class in fig. 1A and B, resp. Neural networks are able to solve this task, in the sense that their classification error *per sample* is below 0.5, implying strong distinguishability of the whole data matrix. Indeed, some of the hidden neurons converge to the spike u of the covariance matrix, as can be seen from the maximum value of the normalised overlaps $\max_k w_k^\top u / \sqrt{\|w_k\| \|u\|}$ in fig. 1C and D, where w_k is the weight vector of the k th hidden neuron. In the linear regime (C), there is an increasingly clear transition from a random overlap for small data sets to a large overlap at large data sets as we increase the input dimension d ; in the quadratic regime (D), the neural network recovers the spike almost perfectly.

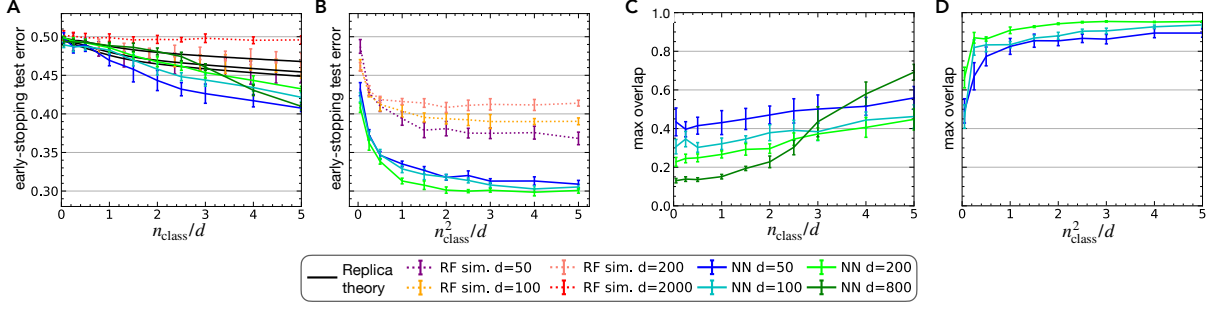


Figure 1: **Learning the spiked Wishart task with neural networks and random features.** (A,B) Test accuracy of random features (RF) and early-stopping test accuracy of two-layer ReLU neural networks (NN) on the spiked Wishart task (eq. 1) with linear and quadratic sample complexity ($n_{\text{class}} \asymp d, d^2$, respectively, where d is the input dimension). Predictions for the performance of random features obtained using replicas are shown in black. (C,D) Maximum normalised overlaps of the hidden neurons in the neural network with the spike u , eq. (1). Parameters: SNR $\beta = 5$. Neural nets and random features have $m = 5d$ hidden neurons. Full experimental details in appendix A.

We also trained *random feature* (RF) models on the task [62–64], where a kernel is approximated by a two-layer neural network where the first-layer weights are fixed at their random initialisation. The performance of random features can be predicted analytically using the replica analysis of Loureiro *et al.* [65] for mixture classification tasks and the Gaussian equivalence theorem for dealing with structured data distributions [66–70] (black lines in fig. 1A, details in appendix C). Replica theory perfectly predicts the performance of random features we obtain in numerical experiments (red-ish dots) for various values of d at linear sample complexity. The key observation is that as we let the input dimension $d \rightarrow \infty$ with m/d and n_{class}/d fixed, the performance of random features tends to random guessing, while at quadratic sample complexity, random features can learn the task, although they perform worse than neural networks. The failure of RF in the linear regime is due to the fact that RF are limited to learning a linear approximation of the target function [71–74] in the linear regime, while the LDLR analysis shows that the target function, i.e. the low-degree likelihood ratio, is a quadratic polynomial. We thus find a clear separation in the sample complexity required by random features ($n_{\text{class}} \gtrsim d^2$) and neural networks ($n_{\text{class}} \gtrsim d$) to learn the spiked Wishart task.

The replica analysis can be extended to the polynomial regime by a simple rescaling of the free energy [75] on several data models, like the vanilla teacher-student setup [76], the Hidden manifold model [66], and vanilla Gaussian mixture classification (see fig. C.1). However, we found that for the spiked Wishart model, the Gaussian equivalence theorem which we need to deal with the random feature distribution *fails* at quadratic sample complexity. This might be due to the fact that in this case, the spike induces a dominant direction in the covariance of the random features, and this direction is also key to solving the task, which can lead to a breakdown of Gaussian equivalence [70]. A similar breakdown of the Gaussian equivalence theorem at quadratic sample complexity has been demonstrated recently in teacher-student setups by Cui *et al.* [77] and Camilli *et al.* [78].

4.2 Spiked cumulant

The LDLR analysis of the spiked cumulant model predicts that a polynomial-time algorithm requires at least a quadratic number of samples to detect non-Gaussianity, and hence to solve the classification task. Indeed, while neither neural networks nor random features achieve a performance better than random guessing at linear sample complexity, neural networks solve the task in the quadratic regime, fig. 2A and B. The maximum overlap between the hidden neurons and the cumulant spike remain constant in the linear regime (fig. 2C); its high value is a consequence of choosing the maximum overlap among $m = 5d$ hidden neurons, which is large even at initialisation, although this overlap does not permit the network to learn the task. In the quadratic regime, the network recovers the cumulant spike almost perfectly,

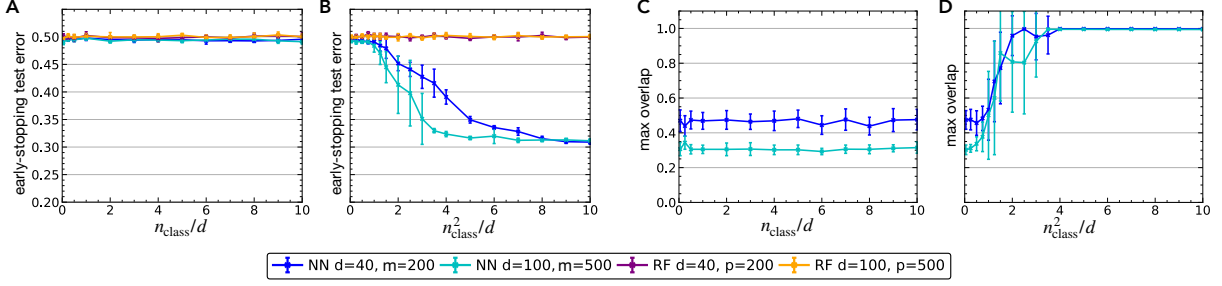


Figure 2: **Learning the spiked cumulant task with neural networks and random features.** (A, B) Test accuracy of random features (RF) and early-stopping test accuracy of two-layer ReLU neural networks (NN) on the spiked cumulant task (eq. 8) with linear and quadratic sample complexity ($n_{\text{class}} \propto d$, d^2 , respectively, where d is the input dimension). (C, D) Maximum normalised overlaps of the hidden neurons in the neural network with the spike u , eq. (8). *Parameters:* SNR $\beta = 10$. Neural nets and random features have $m = 5d$ hidden neurons, same optimisation as in fig. 1. Full experimental details in appendix A.

fig. 2D, resulting in good performance. Random features cannot solve this task even at quadratic sample complexity, since they are limited to a quadratic approximation of the target function [72–74, 79], but we know from the LDLR analysis that the target function is a fourth-order polynomial. We thus find an even larger separation in the minimal number of samples required for random features and neural networks to solve tasks that depend on directions which are encoded exclusively in the higher-order cumulants of the inputs.

4.3 Phase transitions and neural network performance in a simple model for images

We finally show another example of a separation between the performance of random features and neural networks in the feature-learning regime on a toy model for images that was introduced recently by Ingrosso & Goldt [11], the non-linear Gaussian process (NLGP). The idea is to generate inputs that are (i) translation-invariant and that (ii) have sharp edges, both of which are hallmarks of natural images [80]. We first sample a vector $z \in \mathbb{R}^d$ from a normal distribution with zero mean and covariance $C_{ij} = \mathbb{E} z_i z_j = \exp(-|i - j|/\xi)$ to ensure translation-invariance of the inputs, $\xi > 0$. We then introduce edges, i.e. sharp changes in luminosity, by passing z through a saturating non-linearity like the error function,

$$x_i = \text{erf}(gz_i)/Z(g), \quad (18)$$

where $Z(g)$ is a normalisation factor that ensures that the pixel-wise variance $\mathbb{E} x_i^2 = 1$ for all values of the gain $g > 0$. The classification task is to discriminate these “images” from Gaussian inputs with the same mean and covariance, as illustrated in two dimensions in fig. 3A. This task is different from the spiked cumulant model in that the cumulant of the NLGP is not low-rank, so there are many directions that carry a signal about the non-Gaussianity of the inputs.

We trained wide two-layer neural networks on this task and interpolated between the feature learning and the “lazy” regime using the α -renormalisation trick of Chizat *et al.* [81]. As we increase α , the networks go from feature learners ($\alpha = 1$) to an effective random feature model and require an increasing amount of data to solve the task, fig. 3B. There appears to be a sharp transition from random guessing to non-trivial performance as we increase the number of training samples for all values of α . This transition is preceded by a transition in the behaviour of the higher-order cumulant that was reported by Ingrosso & Goldt [11]. They showed numerically that the CP-factors of the empirical fourth-order cumulant T , defined as the vectors $\hat{u} \in \mathbb{R}^d$ that give the best rank- r approximation $\hat{T} = \sum_{k=1}^r \gamma_k \hat{u}_k^{\otimes 4}$ of T [82], localise in space if the data set from which the empirical cumulant is calculated is large enough. Quantifying the localisation of a vector using the *inverse participation ratio*

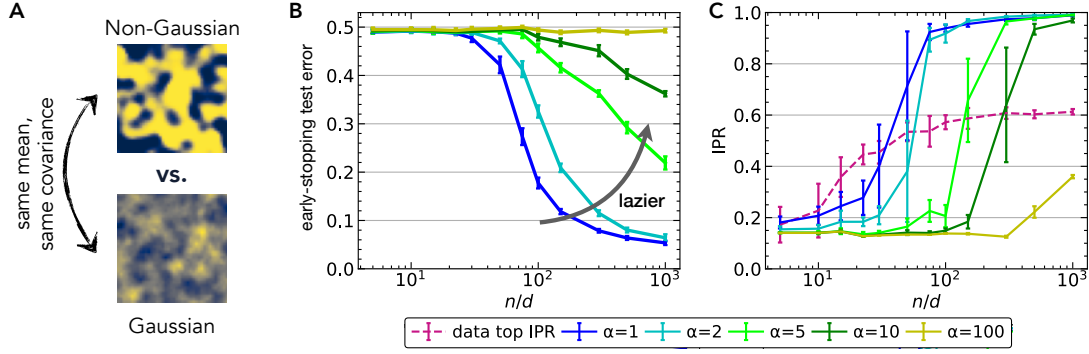


Figure 3: **A phase transition in the fourth-order cumulant precedes learning from the fourth cumulant.** (A) We train neural networks to discriminate inputs sampled from a simple non-Gaussian model for images introduced by Ingrosso & Goldt [11] (top) from Gaussians with the same mean and covariance. (B) Test error of two-layer neural networks interpolating between the fully-trained ($\alpha = 1$) and lazy regimes (large α) using the method of Chizat *et al.* [81] on this task. (C) The inverse participation ratio (19), which is large if a vector is localised, of the leading principal component (“CP-factor”) of the non-Gaussian inputs (dashed purple line) and the maximum IPR of the first-layer weights of the trained networks. Parameters: Gain $g = 3$, $\xi = 1$, $d = 20$, $m = 100$. Full experimental details in appendix A.

(IPR)

$$\text{IPR}(w) = \frac{\sum_{i=1}^d w_i^4}{\left(\sum_{i=1}^d w_i^2\right)^2}, \quad (19)$$

we confirm that the leading CP-factors of the fourth-order cumulant localise (red dashed line in fig. 3C). The localisation of the CP-factors occurs with slightly less samples than the best-performing neural network requires to learn ($\alpha = 1$). The weights of the neural networks also localise. Interestingly, the localisation of the weights always occurs at a sample complexity that is slightly lower than the one at which the neural network starts to solve the task. The laziest network ($\alpha = 100$), i.e. the one where the first layer weights move least and which is hence closest to random features, does not learn the task even with a training set containing $n = 10^3 d$ samples when $d = 20$, indicating again a large advantage of feature learners over methods with fixed feature maps, such as random features.

5 Concluding perspectives

Neural networks crucially rely on the higher-order correlations of their inputs to extract statistical patterns that help them solve their tasks. Here, we have studied the difficulty of learning from higher-order correlations in the spiked cumulant model, where the first non-trivial information in the data set is carried by the input cumulants of order 4 and higher. Our analysis of the corresponding hypothesis test revealed that data sampled from the spiked cumulant model could be statistically distinguishable (in the sense that it passes the *second moment method for distinguishability*) from isotropic Gaussian inputs at linear sample complexity, while the number of samples required to strongly distinguish the two distributions in polynomial time scales as $n \gtrsim d^2$ for a wide class of algorithms, i.e. those covered by the low-degree conjecture [5–8], suggesting the existence of a large statistical-to-computational gap in this problem. Our experiments with neural networks show that they learn from HOCs efficiently in the sense that they match the sample complexities predicted by the analysis of the hypothesis test, which is in stark contrast to random features, which require a lot more data. In the future, it will be intriguing to analyse the *dynamics* of neural networks on the spiked cumulant model or the non-linear Gaussian process more in detail. An outstanding question there would be how neural networks extract information from the higher-order cumulants of realistic data sets efficiently.

Acknowledgements We thank Zhou Fan, Yue Lu, Antoine Maillard, Alessandro Pacco, Subhabrata Sen, Gabriele Sicuro, and Ludovic Stephan for stimulating discussions on various aspects of this work. SG acknowledges co-funding from Next Generation EU, in the context of the National Recovery and Resilience Plan, Investment PE1 – Project FAIR “Future Artificial Intelligence Research”.

Author contributions ES performed the numerical experiments with neural networks and random features. LB performed the (low-degree) likelihood analysis. FG performed the replica analysis of random features. SG designed research and advised ES and LB. All authors contributed to writing the paper.

References

1. Refinetti, M., Ingrosso, A. & Goldt, S. *Neural networks trained with SGD learn distributions of increasing complexity* in *International Conference on Machine Learning* (2023), 28843–28863 (cit. on p. 1).
2. Jacot, A., Gabriel, F. & Hongler, C. *Neural Tangent Kernel: Convergence and Generalization in Neural Networks* in *Advances in Neural Information Processing Systems* (eds Bengio, S. et al.) **31** (Curran Associates, Inc., 2018) (cit. on pp. 2, 3).
3. Arora, S. et al. On exact computation with an infinitely wide neural net. *Advances in neural information processing systems* **32** (2019) (cit. on pp. 2, 3).
4. Geiger, M., Spigler, S., Jacot, A. & Wyart, M. Disentangling feature and lazy training in deep neural networks. *Journal of Statistical Mechanics: Theory and Experiment* **2020**, 113301 (2020) (cit. on pp. 2, 3).
5. Barak, B. et al. A nearly tight sum-of-squares lower bound for the planted clique problem. *SIAM Journal on Computing* **48**, 687–735 (2019) (cit. on pp. 2, 4, 12).
6. Hopkins, S. B. et al. *The power of sum-of-squares for detecting hidden structures* in *IEEE 58th Annual Symposium on Foundations of Computer Science (FOCS)* (2017), 720–731 (cit. on pp. 2, 4, 12).
7. Hopkins, S. B. & Steurer, D. Bayesian estimation from few samples: community detection and related problems. *arXiv:1710.00264* (2017) (cit. on pp. 2, 4, 12).
8. Hopkins, S. *Statistical inference and the sum of squares method* PhD thesis (Cornell University, 2018) (cit. on pp. 2, 4, 5, 12).
9. Baik, J., Ben Arous, G. & Pécché, S. Phase transition of the largest eigenvalue for nonnull complex sample covariance matrices. *The Annals of Probability* **33**, 1643–1697 (2005) (cit. on pp. 2, 3, 5).
10. Potters, M. & Bouchaud, J.-P. *A First Course in Random Matrix Theory: for Physicists, Engineers and Data Scientists* (Cambridge University Press, 2020) (cit. on pp. 2, 3).
11. Ingrosso, A. & Goldt, S. Data-driven emergence of convolutional structure in neural networks. *Proceedings of the National Academy of Sciences* **119**, e2201854119 (2022) (cit. on pp. 2, 11, 12).
12. Paul, D. Asymptotics of sample eigenstructure for a large dimensional spiked covariance model. *Statistica Sinica*, 1617–1642 (2007) (cit. on p. 2).
13. Berthet, Q. & Rigollet, P. Optimal detection of sparse principal components in high dimension. *The Annals of Statistics* (2012) (cit. on p. 2).
14. Berthet, Q. & Rigollet, P. Complexity theoretic lower bounds for sparse principal component detection in *Conference on Learning Theory (COLT)* (2013) (cit. on p. 2).
15. Lesieur, T., Krzakala, F. & Zdeborová, L. Phase transitions in sparse PCA in *2015 IEEE International Symposium on Information Theory (ISIT)* (2015), 1635–1639 (cit. on p. 2).

16. Lesieur, T., Krzakala, F. & Zdeborová, L. *MMSE of probabilistic low-rank matrix estimation: Universality with respect to the output channel* in 2015 53rd Annual Allerton Conference on Communication, Control, and Computing (Allerton) (2015), 680–687 (cit. on p. 2).
17. Perry, A., Wein, A. S., Bandeira, A. S. & Moitra, A. Optimality and sub-optimality of PCA for spiked random matrices and synchronization. *arXiv:1609.05573* (2016) (cit. on pp. 2, 4).
18. Krzakala, F., Xu, J. & Zdeborová, L. *Mutual information in rank-one matrix estimation* in 2016 IEEE Information Theory Workshop (ITW) (2016), 71–75 (cit. on p. 2).
19. Dia, M., Macris, N., Krzakala, F., Lesieur, T., Zdeborová, L. *et al.* Mutual information for symmetric rank-one matrix estimation: A proof of the replica formula. *Advances in Neural Information Processing Systems* **29** (2016) (cit. on p. 2).
20. Miolane, L. Phase transitions in spiked matrix estimation: information-theoretic analysis. *arXiv:1806.04343* (2018) (cit. on p. 2).
21. Lelarge, M. & Miolane, L. Fundamental limits of symmetric low-rank matrix estimation. *Probability Theory and Related Fields* **173**, 859–929 (2019) (cit. on p. 2).
22. El Alaoui, A., Krzakala, F. & Jordan, M. Fundamental limits of detection in the spiked Wigner model. *The Annals of Statistics* **48**, 863–885 (2020) (cit. on p. 2).
23. Richard, E. & Montanari, A. A statistical model for tensor PCA. *Advances in neural information processing systems* **27** (2014) (cit. on pp. 2, 9).
24. Hopkins, S. B., Shi, J. & Steurer, D. *Tensor principal component analysis via sum-of-square proofs* in Conference on Learning Theory (2015), 956–1006 (cit. on p. 2).
25. Montanari, A., Reichman, D. & Zeitouni, O. On the limitation of spectral methods: From the gaussian hidden clique problem to rank-one perturbations of gaussian tensors. *Advances in Neural Information Processing Systems* **28** (2015) (cit. on pp. 2, 4).
26. Perry, A., Wein, A. S. & Bandeira, A. S. Statistical limits of spiked tensor models. *arXiv:1612.07728* (2016) (cit. on pp. 2, 9).
27. Kim, C., Bandeira, A. S. & Goemans, M. X. *Community detection in hypergraphs, spiked tensor models, and sum-of-squares* in 2017 International Conference on Sampling Theory and Applications (SampTA) (2017), 124–128 (cit. on p. 2).
28. Lesieur, T., Miolane, L., Lelarge, M., Krzakala, F. & Zdeborová, L. *Statistical and computational phase transitions in spiked tensor estimation* in 2017 IEEE International Symposium on Information Theory (ISIT) (2017), 511–515 (cit. on pp. 2, 9).
29. Arous, G. B., Gheissari, R. & Jagannath, A. Algorithmic thresholds for tensor PCA. *The Annals of Probability* **48**, 2052–2087 (2020) (cit. on p. 2).
30. Jagannath, A., Lopatto, P. & Miolane, L. Statistical thresholds for tensor PCA. *The Annals of Applied Probability* **30**, 1910–1933 (2020) (cit. on pp. 2, 7).
31. Niles-Weed, J. & Rigollet, P. Estimation of wasserstein distances in the spiked transport model. *Bernoulli* **28**, 2663–2688 (2022) (cit. on p. 2).
32. Zdeborová, L. & Krzakala, F. Statistical physics of inference: Thresholds and algorithms. *Advances in Physics* **65**, 453–552 (2016) (cit. on p. 2).
33. Lesieur, T., Krzakala, F. & Zdeborová, L. Constrained low-rank matrix estimation: Phase transitions, approximate message passing and applications. *Journal of Statistical Mechanics: Theory and Experiment* **2017**, 073403 (2017) (cit. on p. 2).
34. Bandeira, A. S., Perry, A. & Wein, A. S. Notes on computational-to-statistical gaps: predictions using statistical physics. *Portugaliae mathematica* **75**, 159–186 (2018) (cit. on p. 2).

35. Kunisky, D., Wein, A. S. & Bandeira, A. S. *Notes on computational hardness of hypothesis testing: Predictions using the low-degree likelihood ratio* in *ISAAC Congress (International Society for Analysis, its Applications and Computation)* (2019), 1–50 (cit. on pp. 2, 4, 5, 9, 22).
36. Wang, C. & Lu, Y. M. *The Scaling Limit of High-Dimensional Online Independent Component Analysis* in *Advances in neural information processing systems* **31** (2017) (cit. on pp. 2, 3, 5).
37. Hyvärinen, A. & Oja, E. Independent component analysis: algorithms and applications. *Neural networks* **13**, 411–430 (2000) (cit. on p. 3).
38. Li, Y. & Yuan, Y. Convergence analysis of two-layer neural networks with relu activation. *Advances in neural information processing systems* **30** (2017) (cit. on p. 3).
39. Du, S., Zhai, X., Póczos, B. & Singh, A. *Gradient Descent Provably Optimizes Over-parameterized Neural Networks* in *International Conference on Learning Representations* (2019) (cit. on p. 3).
40. Li, Y. & Liang, Y. *Learning Overparameterized Neural Networks via Stochastic Gradient Descent on Structured Data* in *Advances in Neural Information Processing Systems* **31** (2018) (cit. on p. 3).
41. Allen-Zhu, Z., Li, Y. & Song, Z. *A convergence theory for deep learning via over-parameterization* in *International Conference on Machine Learning* (2019), 242–252 (cit. on p. 3).
42. Bordelon, B., Canatar, A. & Pehlevan, C. *Spectrum dependent learning curves in kernel regression and wide neural networks* in *International Conference on Machine Learning* (2020), 1024–1034 (cit. on p. 3).
43. Canatar, A., Bordelon, B. & Pehlevan, C. Spectral bias and task-model alignment explain generalization in kernel regression and infinitely wide neural networks. *Nature communications* **12**, 2914 (2021) (cit. on p. 3).
44. Nguyen, Q., Mondelli, M. & Montufar, G. F. *Tight bounds on the smallest eigenvalue of the neural tangent kernel for deep relu networks* in *International Conference on Machine Learning* (2021), 8119–8129 (cit. on p. 3).
45. Bach, F. Breaking the curse of dimensionality with convex neural networks. *The Journal of Machine Learning Research* **18**, 629–681 (2017) (cit. on p. 3).
46. Ghorbani, B., Mei, S., Misiakiewicz, T. & Montanari, A. *Limitations of Lazy Training of Two-layers Neural Network* in *Advances in Neural Information Processing Systems* **32** (2019), 9111–9121 (cit. on p. 3).
47. Ghorbani, B., Mei, S., Misiakiewicz, T. & Montanari, A. *When do neural networks outperform kernel methods?* in *Advances in Neural Information Processing Systems* **33** (2020) (cit. on p. 3).
48. Chizat, L. & Bach, F. *Implicit bias of gradient descent for wide two-layer neural networks trained with the logistic loss* in *Conference on Learning Theory* (2020), 1305–1338 (cit. on p. 3).
49. Daniely, A. & Malach, E. Learning parities with neural networks. *Advances in Neural Information Processing Systems* **33**, 20356–20365 (2020) (cit. on p. 3).
50. Paccolat, J., Petrini, L., Geiger, M., Tyloo, K. & Wyart, M. Geometric compression of invariant manifolds in neural networks. *Journal of Statistical Mechanics: Theory and Experiment* **2021**, 044001 (2021) (cit. on p. 3).
51. Yehudai, G. & Shamir, O. *On the Power and Limitations of Random Features for Understanding Neural Networks* in *Advances in Neural Information Processing Systems* **32** (2019), 6598–6608 (cit. on p. 3).
52. Refinetti, M., Goldt, S., Krzakala, F. & Zdeborová, L. *Classifying high-dimensional gaussian mixtures: Where kernel methods fail and neural networks succeed* in *International Conference on Machine Learning* (2021), 8936–8947 (cit. on p. 3).
53. Banks, J., Moore, C., Neeman, J. & Netrapalli, P. *Information-theoretic thresholds for community detection in sparse networks* in *Conference on Learning Theory* (2016), 383–416 (cit. on p. 4).

54. Kesten, H. & Stigum, B. P. Additional limit theorems for indecomposable multidimensional Galton-Watson processes. *The Annals of Mathematical Statistics* **37**, 1463–1481 (1966) (cit. on p. 4).
55. Decelle, A., Krzakala, F., Moore, C. & Zdeborová, L. Inference and phase transitions in the detection of modules in sparse networks. *Physical Review Letters* **107**, 065701 (2011) (cit. on p. 4).
56. Decelle, A., Krzakala, F., Moore, C. & Zdeborová, L. Asymptotic analysis of the stochastic block model for modular networks and its algorithmic applications. *Physical review E* **84**, 066106 (2011) (cit. on p. 4).
57. Bandeira, A. S., Kunisky, D. & Wein, A. S. *Computational Hardness of Certifying Bounds on Constrained PCA Problems* in *11th Innovations in Theoretical Computer Science Conference (ITCS 2020)* (ed Vidick, T.) **151** (Schloss Dagstuhl–Leibniz-Zentrum fuer Informatik, 2020), 78:1–78:29 (cit. on pp. 5, 21–23).
58. Baldi, P. & Chauvin, Y. Temporal evolution of generalization during learning in linear networks. *Neural Computation* **3**, 589–603 (1991) (cit. on p. 6).
59. Le Cun, Y., Kanter, I. & Solla, S. A. Eigenvalues of covariance matrices: Application to neural-network learning. *Physical Review Letters* **66**, 2396 (1991) (cit. on p. 6).
60. Saxe, A. M., McClelland, J. L. & Ganguli, S. *Exact solutions to the nonlinear dynamics of learning in deep linear neural networks* in *ICLR* (2014) (cit. on p. 6).
61. Advani, M. S., Saxe, A. M. & Sompolinsky, H. High-dimensional dynamics of generalization error in neural networks. *Neural Networks* **132**, 428–446 (2020) (cit. on p. 6).
62. Balcan, M.-F., Blum, A. & Vempala, S. Kernels as features: On kernels, margins, and low-dimensional mappings. *Machine Learning* **65**, 79–94 (2006) (cit. on pp. 9, 10).
63. Rahimi, A. & Recht, B. *Random features for large-scale kernel machines* in *Advances in neural information processing systems* (2008), 1177–1184 (cit. on pp. 9, 10, 18).
64. Rahimi, A. & Recht, B. *Weighted sums of random kitchen sinks: Replacing minimization with randomization in learning* in *Advances in neural information processing systems* (2009), 1313–1320 (cit. on pp. 9, 10, 18).
65. Loureiro, B. *et al.* Learning gaussian mixtures with generalized linear models: Precise asymptotics in high-dimensions. *Advances in Neural Information Processing Systems* **34**, 10144–10157 (2021) (cit. on pp. 10, 36, 37).
66. Goldt, S., Mézard, M., Krzakala, F. & Zdeborová, L. Modeling the influence of data structure on learning in neural networks: The hidden manifold model. *Physical Review X* **10**, 041044 (2020) (cit. on pp. 10, 36).
67. Gerace, F., Loureiro, B., Krzakala, F., Mézard, M. & Zdeborová, L. *Generalisation error in learning with random features and the hidden manifold model* in *International Conference on Machine Learning* (2020), 3452–3462 (cit. on pp. 10, 36, 37).
68. Hu, H. & Lu, Y. M. Universality laws for high-dimensional learning with random features. *IEEE Transactions on Information Theory* **69**, 1932–1964 (2022) (cit. on pp. 10, 36).
69. Mei, S. & Montanari, A. The generalization error of random features regression: Precise asymptotics and the double descent curve. *Communications on Pure and Applied Mathematics* **75**, 667–766 (2022) (cit. on pp. 10, 36).
70. Goldt, S. *et al.* *The gaussian equivalence of generative models for learning with shallow neural networks* in *Mathematical and Scientific Machine Learning* (2022), 426–471 (cit. on pp. 10, 36).
71. Ghorbani, Mei, S., Misiakiewicz, T. & Montanari, A. "Linearized two-layers neural networks in high dimension." *Annals of Statistics* **49**, 1029–1054 (2021) (cit. on p. 10).
72. Xiao, L., Hu, H., Misiakiewicz, T., Lu, Y. & Pennington, J. Precise Learning Curves and Higher-Order Scalings for Dot-product Kernel Regression. *Advances in Neural Information Processing Systems* **35**, 4558–4570 (2022) (cit. on pp. 10, 11).

73. Mei, S., Misiakiewicz, T. & Montanari, A. Generalization error of random feature and kernel methods: Hypercontractivity and kernel matrix concentration. *Applied and Computational Harmonic Analysis* **59**, 3–84 (2022) (cit. on pp. 10, 11).
74. Misiakiewicz, T. & Montanari, A. Six lectures on linearized neural networks. *arXiv:2308.13431* (2023) (cit. on pp. 10, 11).
75. Dietrich, R., Oppen, M. & Sompolinsky, H. Statistical mechanics of support vector networks. *Physical review letters* **82**, 2975 (1999) (cit. on pp. 10, 37).
76. Gardner, E. & Derrida, B. Three unfinished works on the optimal storage capacity of networks. *Journal of Physics A: Mathematical and General* **22**, 1983 (1989) (cit. on p. 10).
77. Cui, H., Krzakala, F. & Zdeborova, L. Bayes-optimal learning of deep random networks of extensive-width in *International Conference on Machine Learning* (2023), 6468–6521 (cit. on p. 10).
78. Camilli, F., Tieplov, D. & Barbier, J. Fundamental limits of overparametrized shallow neural networks for supervised learning. *arXiv preprint arXiv:2307.05635* (2023) (cit. on p. 10).
79. Hu, H. & Lu, Y. M. Sharp asymptotics of kernel ridge regression beyond the linear regime. *arXiv:2205.06798* (2022) (cit. on p. 11).
80. Bell, A. & Sejnowski, T. J. *Edges are the 'Independent Components' of Natural Scenes*. in *Advances in Neural Information Processing Systems* (eds Mozer, M., Jordan, M. & Petsche, T.) **9** (MIT Press, 1996) (cit. on p. 11).
81. Chizat, L., Oyallon, E. & Bach, F. *On Lazy Training in Differentiable Programming* in *Advances in Neural Information Processing Systems* (eds Wallach, H. et al.) **32** (Curran Associates, Inc., 2019) (cit. on pp. 11, 12, 18).
82. Kolda, T. G. & Bader, B. W. Tensor Decompositions and Applications. *SIAM Review* **51**, 455–500 (2009) (cit. on p. 11).
83. Pedregosa, F. et al. Scikit-learn: Machine Learning in Python. *Journal of Machine Learning Research* **12**, 2825–2830 (2011) (cit. on p. 18).
84. Kossaifi, J., Panagakis, Y., Anandkumar, A. & Pantic, M. TensorLy: Tensor Learning in Python. *Journal of Machine Learning Research (JMLR)* **20** (2019) (cit. on p. 18).
85. McCullagh, P. *Tensor methods in statistics* (Courier Dover Publications, 2018) (cit. on pp. 19, 21, 31).
86. Szegő, G. *Orthogonal Polynomials* (American mathematical society, 1939) (cit. on p. 19).
87. Abramowitz, M. & Stegun, I. A. *Handbook of mathematical functions with formulas, graphs, and mathematical tables* xiv+1046 (National Bureau of Standards, 1964) (cit. on p. 19).
88. Lukacs, E. A Survey of the Theory of Characteristic Functions. *Advances in Applied Probability* **4**, 1–38 (1972) (cit. on p. 21).

Appendix

A Experimental details

A.1 Figures 1, 2

For the spiked Wishart and spiked cumulant tasks, we trained two-layer ReLU neural networks $\phi_\theta(x) = v^\top \max(0, w^\top x)$. The number of hidden neurons $m = 5d$, where d is the input dimension. We train the networks using SGD with a learning rate of 0.002 and a weight-decay of 0.002 for 50 epochs for the spiked Wishart task and for 200 epochs for the spiked cumulant task. The plots show the early-stopping test errors. The results are plotted as averages over 10 random seeds.

The random features (RF) models [63, 64] have also a width of $5d$. The ridge regression is performed using scikit-learn [83] with a regularisation of 0.1.

For the spiked datasets, the spikes are from the Rademacher distribution, using a signal-to-noise ratio of 5.0 for the spiked Wishart and 10.0 for the spiked cumulant datasets. For the spike-feature overlaps, we plot the highest overlap amongst the incoming weights of the hidden neurons with the spike, calculated as the normalised dot product.

A.2 Figure 3

For the NLGP-GP task, we use the α -scaling trick of Chizat *et al.* [81] to interpolate between feature- and lazy-learning. We define the network function as:

$$\phi_{\text{NN}}(x; v, W, v_0, W_0) = \frac{\alpha}{K} \left[\sum_j^m v_j \sigma \left(\sum_i^d w_i x_i \right) - \sum_j^m v_{0,j} \sigma \left(\sum_i^d w_{0,i} x_i \right) \right] \quad (\text{A.1})$$

where v_0, w_0 are kept fixed at their initial values. The mean-squared loss is also rescaled by $(1/\alpha^2)$. Changing α from low to high allows to interpolate between the feature- and the lazy-learning limits as the first-layer weights will move away less from their initial values.

For fig. 3, the network has a width of 100 and the optimisation is run by SGD for 200 epochs with a weight-decay of $5 \cdot 10^{-6}$ and learning rate of 0.5. The one-dimensional data vectors have a length of 20; the correlation length is 1 and the signal-to-noise ratio is set to 3. The error shown is early-stopping test error. The localisation of the neural networks' features and the data's fourth moments is shown by the IPR measure (eq. (19)). For the neural networks, the highest IPR is shown amongst the incoming features of the hidden neurons at the final state of the training. For the data, the highest IPR is the highest amongst the CP-factors of the fourth cumulants of the nlgp-class using a rank-1 PARAFAC decomposition from the tensorly package [84].

B Mathematical details on the hypothesis testing problems

In this section, we provide more technical details on Hermite polynomials, LR and LDLR, and present the complete proofs all theorems stated in the main.

B.1 Background

B.1.1 Notation

We use the convention $0 \in \mathbb{N}$. $n \in \mathbb{N}$ denotes the number of samples, d the dimensionality of each data point x . The letters k, m usually denote free natural parameters. Let $[n] := \{1, \dots, n\}$, $\mu \in [n]$ is an index that ranges on the samples and $i \in [d]$ usually ranges on the data dimension. Underlined letters $\underline{x}, \underline{\mathbb{P}}, \underline{\mathbb{Q}}$ are used for objects that are $n \times d$ dimensional. In proofs the letter C denotes numerical constants whose precise value may change from line to line, and any dependency is denoted as a subscript. $m!$

denotes factorial and $m!!$ denotes the double factorial (product of all the numbers $k \leq m$ with the same parity as m).

Multi-index notation We will need multi-index notation to deal with d -dimensional functions and polynomials. Bold greek letters are used to denote multi-indices and their components, $\alpha = (\alpha_1, \dots, \alpha_d) \in \mathbb{N}^d$. The following conventions are adopted:

$$|\alpha| := \sum_{i=1}^d \alpha_i, \quad \alpha! := \prod_{i=1}^d \alpha_i!, \quad x^\alpha := \prod_{i=1}^d x_i^{\alpha_i} \quad (B.1)$$

$$\partial_\alpha f(x_1, \dots, x_d) = \frac{\partial}{\partial x^\alpha} f := \left(\frac{\partial}{\partial x_1^{\alpha_1}} \cdots \frac{\partial}{\partial x_d^{\alpha_d}} \right) f$$

Since we will have n samples of d -dimensional variables, we will need to consider polynomials and functions in nd variables. To deal with all these variables we introduce multi-multi indices (denoted by underlined bold Greek letters $\underline{\alpha}, \underline{\beta}, \dots$). They are $n \times d$ matrices in with entries in \mathbb{N} (i.e. elements of $\mathbb{N}^{n \times d}$)

$$\underline{\alpha} := (\alpha_i^\mu) = \begin{pmatrix} \alpha_1^1 & \cdots & \alpha_d^1 \\ \vdots & \ddots & \vdots \\ \alpha_1^n & \cdots & \alpha_d^n \end{pmatrix} \quad (B.2)$$

We denote by α^μ the rows of $\underline{\alpha}$, that are d -dimensional multi-indices.

All the notations (B.1) generalize to multi-multi-indices in the following way:

$$|\underline{\alpha}| := \sum_{\mu=1}^n |\alpha^\mu| = \sum_{\mu=1}^n \sum_{i=1}^d \alpha_i^\mu, \quad \underline{\alpha}! := \prod_{\mu} \alpha^\mu! = \prod_{\mu} \prod_i \alpha_i^{\mu!}, \quad (B.3)$$

$$\underline{x}^{\underline{\alpha}} := \prod_{\mu=1}^n (x^\mu)^{\alpha^\mu} = \prod_{\mu=1}^n \prod_{i=1}^d (x_i^\mu)^{\alpha_i^\mu}$$

$$\partial_{\underline{\alpha}} f(\underline{x}) := \left(\frac{\partial}{\partial (x^1)^{\alpha^1}} \cdots \frac{\partial}{\partial (x^n)^{\alpha^n}} \right) f(\underline{x})$$

B.1.2 Hermite Polynomials

We recall here the definitions and key properties of the Hermite polynomials.

Definition B.1. The Hermite polynomial of degree m is defined as

$$h_m(x) := (-1)^m e^{\frac{x^2}{2}} \frac{d^m}{dx^m} \left(e^{-\frac{x^2}{2}} \right) \quad (B.4)$$

Here is a list of the first 5 Hermite polynomials:

$$\begin{aligned} h_0(x) &= 1 \\ h_1(x) &= x \\ h_2(x) &= x^2 - 1 \\ h_3(x) &= x^3 - 3x \\ h_4(x) &= x^4 - 6x^2 + 3 \end{aligned} \quad (B.5)$$

The Hermite polynomials enjoy the following properties that we will use in the subsequent proofs (for details see section 5.4 in McCullagh [85], Szegő [86] and Abramowitz & Stegun [87]):

- they are orthogonal with respect to the L^2 product weighted with the density of the Normal distribution:

$$\frac{1}{\sqrt{2\pi}} \int_{-\infty}^{\infty} h_n(x) h_m(x) e^{-\frac{x^2}{2}} dx = n! \delta_{m,n}; \quad (\text{B.6})$$

- h_m is a monic polynomial of degree m , hence $(h_m)_{m \in \{1, \dots, N\}}$ generates the space of polynomials of degree $\leq N$;
- the previous two properties imply that the family of Hermite polynomials is an orthogonal basis for the Hilbert space $L^2(\mathbb{R}, \mathbb{Q})$ where \mathbb{Q} is the normal distribution;
- they enjoy the following recurring relationship

$$h_{m+1}(x) = x h_m(x) - h'_m(x), \quad (\text{B.7})$$

which can also be expressed as a relationship between coefficients as follows. If $h_m(x) = \sum_{k=0}^m a_{m,k} x^k$, then

$$a_{m+1,k} = \begin{cases} -a_{m,1} & k = 0, \\ a_{m,k-1} - (k+1)a_{m,k+1} & k > 0. \end{cases} \quad (\text{B.8})$$

They also satisfy identities of binomial type, like:

$$h_m(x+y) = \sum_{k=0}^m \binom{m}{k} x^{m-k} h_k(y) \quad (\text{B.9})$$

$$h_m(\gamma x) = \sum_{j=0}^{\lfloor m/2 \rfloor} \gamma^{m-2j} (\gamma^2 - 1)^j \binom{m}{2j} (2j-1)!! h_{m-2j}(x) \quad (\text{B.10})$$

Multivariate case In the multivariate m -dimensional case we can consider Hermite tensors $(H_\alpha)_{\alpha \in \mathbb{N}^m}$ defined as:

$$H_\alpha(x_1, \dots, x_m) = \prod_{i=1}^m h_{\alpha_i}(x_i) \quad (\text{B.11})$$

all the properties of the one-dimensional Hermite polynomials generalize to this case, in particular they form an orthogonal basis of $L^2(\mathbb{R}^m, \mathbb{Q})$ where \mathbb{Q} is a multivariate normal distribution. If $\langle \cdot, \cdot \rangle$ is the inner product of that Hilbert space, we have that:

$$\langle H_\alpha, H_\beta \rangle = \alpha! \delta_{\alpha,\beta} \quad (\text{B.12})$$

Of course all this is valid in the case $m = nd$, where we can also use multi-multi indices to get the following identity:

$$H_{\underline{\alpha}}(x_1^1, \dots, x_d^n) = \prod_{\mu=1}^n H_{\alpha^\mu}(x^\mu) = \prod_{\mu=1}^n \prod_{i=1}^d h_{\alpha_i^\mu}(x_i^\mu) \quad (\text{B.13})$$

We are now ready to see the proof of eq. (B.51).

Lemma B.2. *We consider a hypothesis testing problem in \mathbb{R}^d where the null hypothesis \mathbb{Q} is the multivariate Gaussian distribution $\mathcal{N}(0, \mathbb{1}_{d \times d})$, while the alternative hypothesis \mathbb{P} is absolutely continuous with respect to it. Then:*

$$L^{\leq D} = \sum_{|\alpha| \leq D} \frac{\langle L, H_\alpha \rangle H_\alpha}{\alpha!} = \sum_{|\alpha| \leq D} \frac{\mathbb{E}_{x \sim \mathbb{P}}[H_\alpha(x)] H_\alpha}{\alpha!} \quad (\text{B.14})$$

Which implies

$$\|L^{\leq D}\|^2 = \sum_{|\alpha| \leq D} \frac{\langle L, H_\alpha \rangle^2}{\alpha!} = \sum_{|\alpha| \leq D} \frac{\mathbb{E}_{x \sim \mathbb{P}}[H_\alpha(x)]^2}{\alpha!} \quad (\text{B.15})$$

Proof. First note that

$$\langle L, H_\alpha \rangle = \mathbb{E}_{x \sim \mathbb{P}} [H_\alpha(x)] \quad (\text{B.16})$$

due to the definition of likelihood ratio and a change of variable in the expectation. Then we can just use the fact that $(H_\alpha)_\alpha \in \mathbb{N}^d$ are an orthogonal basis for $L^2(\mathbb{R}^d, \mathbb{Q})$, and if we consider the Hermite polynomials up to degree D , they are also a basis of the space of polynomials in which we want to project L to get $L^{\leq D}$. Hence the formulas follow by just computing the projection using this basis. \square

Note that we set the lemma in \mathbb{R}^d , but of course it holds also in \mathbb{R}^{nd} just switching to multi-multi index notation.

B.1.3 Hermite coefficients

Lemma B.2 translates the problem of computing the norm of the LDLR to the problem of computing the projections $\langle L, H_\alpha \rangle$. Note that this quantity is equal to $\mathbb{E}_{\mathbb{P}}[H_\alpha(x)]$, which we will call α -th Hermite coefficient of the distribution \mathbb{P} .

The following lemma from [57] provides a version of the integration by parts technique that is tailored for Hermite polynomials.

Lemma B.3. *Let $f : \mathbb{R}^d \rightarrow \mathbb{R}^d$ be a function that is continuously differentiable k times. Assume that f and all of its partial derivatives up to order k are bounded by $O(\exp(|y|^\lambda))$ for some $\lambda \in (0, 2)$, then for any $\alpha \in \mathbb{N}^d$ such that $|\alpha| \leq k$*

$$\langle f, H_\alpha \rangle = \mathbb{E}_{y \sim \mathcal{N}(0, \mathbb{I})} [H_\alpha(y) f(y)] = \mathbb{E}_{y \sim \mathcal{N}(0, \mathbb{I})} [\partial_\alpha f(y)] \quad (\text{B.17})$$

Proof. eq. (B.17) can be proved by doing induction on k using eq. (B.7), see [57] for details. \square

B.1.4 Links with cumulant theory

The cumulants $(\kappa_\alpha)_{\alpha \in \mathbb{N}^d}$ of a random variable $x \in \mathbb{R}^d$, can be defined as the Taylor coefficients of the expansion in ξ of the *cumulant generating function*:

$$K_x(\xi) := \log \left(\mathbb{E} \left[e^{\xi \cdot x} \right] \right) \quad (\text{B.18})$$

Order one cumulant is the mean, order two is the variance, and higher order cumulants encode more complex correlations among the variables. The Gaussian distribution is the only non constant distribution to have a polynomial cumulant generating function (as proved in theorem 7.3.5 in [88]), if $z \sim \mathcal{N}(\mu, \Sigma)$, then:

$$K_z(\xi) = \mu \xi + \frac{1}{2} \xi^\top \Sigma \xi.$$

Hence cumulants with order higher than three can also be seen as a measure of how much a distribution deviates from Gaussianity (i.e how much it deviates from its best Gaussian approximation)

On this point the similarity with Hermite coefficients is evident. Indeed, up to order five, on whitened distributions, cumulants and Hermite coefficients coincide. But from sixth order onward, they start diverging. They are still linked by deterministic relationship, but its combinatorial complexity increases swiftly and it is not easy to translate formulas involving Hermite coefficients into cumulants and vice versa. For this reason, our low-degree analysis of the likelihood ratio leading to theorem 3.3 keeps the formalism that naturally arises from the computations, which is based on Hermite coefficients. A detailed discussion of the relation between Hermite polynomials and cumulants in the context of asymptotic expansions of distributions like the Gram-Charlier and Edgeworth series can be found in chapter 5 McCullagh [85].

B.2 LDLR analysis of the spiked Wishart model

Here we prove theorem 2.4 on the hypothesis testing problem for the spiked Wishart model, where we consider the following hypotheses:

- \mathbb{Q} (Null hypothesis): $x = z$
- \mathbb{P} (Alternative hypothesis): $x = \sqrt{\frac{\beta}{d}}gu + z$

where z is d -dimensional Gaussian noise, $u \in U$ is a d -dimensional spike vector that follows a prior \mathcal{P} , g is a scalar Gaussian random variable and $\beta > 0$ the signal-to-noise ratio. After drawing the spike u from \mathcal{P} , we take the sample $(x^\mu)_{\mu=1,\dots,n}$, made by i.i.d. variables taken from either $\mathbb{P}(\cdot|u)$ or \mathbb{Q} . The aim is to understand under which conditions on n/d (with $n, d \rightarrow +\infty$) and β , it is possible to find out which distribution the samples were drawn from.

As mentioned in the main text, a thorough LDLR analysis of a more general model that encompasses the spiked Wishart model was performed by Bandeira *et al.* [57]. Their theorem 3.2 is a more general version of our theorem theorem 2.4, that generalizes it in two directions: it works for a class of subgaussian priors on u that satisfy some concentration property, and also allows for negative SNR (the requirement is $\beta > -1$). For completeness, here we show that this result can be obtained as a straightforward application of a Gaussian additive model.

B.2.1 Proof of theorem 2.4

We note that the problem belongs to the class of *Additive Gaussian Noise models* which is studied in depth by Kunisky *et al.* [35]. In those models the two hypotheses have to be expressed as an additive perturbation of white noise:

- \mathbb{P}_n : $\underline{x}_n = y_n + z_n$,
- \mathbb{Q}_n : $\underline{x}_n = z_n$,

The spiked Wishart model that we consider belongs to this class. It can be seen by defining $\mathbb{R}^{nd} \ni y_n = \left(\sqrt{\frac{\beta}{d}}g^1u, \dots, \sqrt{\frac{\beta}{d}}g^nu \right)^\top$. So we can apply theorem 2.6 from Kunisky *et al.* [35], that computes the norm of the LDLR by using two independent replicas of the variable y . Denoting the two replicas by \hat{y} and \tilde{y} , we get

$$\begin{aligned}
\|L_n^{\leq D}\|^2 &= \mathbb{E} \left[\sum_{m=0}^D \frac{1}{m!} (\hat{y} \cdot \tilde{y})^m \right] \\
&= \mathbb{E} \left[\sum_{m=0}^D \frac{\beta^m}{m!d^m} \left(\sum_{\mu=1}^n \hat{g}^\mu \tilde{g}^\mu \hat{u} \cdot \tilde{u} \right)^m \right] \\
&= \sum_{m=0}^D \frac{\beta^m}{m!d^m} \mathbb{E} \left[(\hat{u} \cdot \tilde{u})^m \left(\sum_{\mu=1}^n \hat{g}^\mu \tilde{g}^\mu \right)^m \right] \\
&= \sum_{m=0}^D \frac{\beta^m}{m!d^m} \mathbb{E} \left[\left(\sum_{\mu=1}^n \hat{g}^\mu \tilde{g}^\mu \right)^m \right] \mathbb{E} [(\hat{u} \cdot \tilde{u})^m]
\end{aligned} \tag{B.19}$$

Note now that $\sum_{\mu=1}^n \hat{g}^\mu \tilde{g}^\mu$ has the same distribution as $-\sum_{\mu=1}^n \hat{g}^\mu \tilde{g}^\mu$, so its distribution is even and all the odd moments are 0. This means that we can reduce to the case $m = 2k$, so we need to study:

$$\|L_n^{\leq D}\|^2 = \sum_{k=0}^{\lfloor D/2 \rfloor} \frac{\beta^{2k}}{(2k)!d^{2k}} \underbrace{\mathbb{E} \left[\left(\sum_{\mu=1}^n \hat{g}^\mu \tilde{g}^\mu \right)^{2k} \right]}_{T_1} \underbrace{\mathbb{E} [(\hat{u} \cdot \tilde{u})^{2k}]}_{T_2} \tag{B.20}$$

Let us consider the term T_1 . Call $Y^\mu := \hat{g}^\mu \tilde{g}^\mu$. The distribution of each of the Y^μ is not Gaussian, but we have that $\mathbb{E}[Y^\mu] = 0$ and $\text{Var}(Y^\mu) = 1$. So by the central limit theorem $S_n := \frac{1}{\sqrt{n}} \sum_{\mu=1}^n Y^\mu$ converges to a standard normal in distribution, as $n \rightarrow \infty$. Note that the cumulants of S_n can be computed thanks to linearity and additivity of cumulants and are $\kappa_{2k}^{(S_n)} = n^{1-k} \kappa_{2k}^Y$. So they all go to 0 except from the variance. Since the moments can be written as a function of the cumulants up to that order, it follows that $\lim_n \mathbb{E}[S_n^{2k}]$ will be the $2k$ -th moment of the standard normal distribution, which means that we have the following:

$$\lim_{n \rightarrow +\infty} \mathbb{E} \left[\left(\frac{1}{\sqrt{n}} \sum_{\mu=1}^n \hat{g}^\mu \tilde{g}^\mu \right)^{2k} \right] = (2k-1)!! \quad (\text{B.21})$$

We turn now to T2 and do the same reasoning. Define $v_i := \hat{u}_i \tilde{u}_i$, both in Rademacher and in Gaussian prior case, we have that the $(v_i)_{i=1, \dots, d}$ is an independent family of random variables that have 0 mean and variance equal to 1. So we can again apply the central limit theorem to get that:

$$\lim_{d \rightarrow +\infty} \mathbb{E} \left[\left(\frac{\hat{u} \cdot \tilde{u}}{\sqrt{d}} \right)^{2k} \right] = (2k-1)!! \quad (\text{B.22})$$

Taking the limit for $n, d \rightarrow +\infty$ with the constraint $\gamma = d/n$, we have that:

$$\begin{aligned} \lim_{n, d \rightarrow \infty} \|L_n^{\leq D}\|^2 &= \lim_{n, d \rightarrow \infty} \sum_{k=0}^{\lfloor D/2 \rfloor} \frac{\beta^{2k} n^k}{(2k)! d^k} \mathbb{E} \left[\left(\frac{1}{\sqrt{n}} \sum_{\mu=1}^n \hat{g}^\mu \tilde{g}^\mu \right)^{2k} \right] \mathbb{E} \left[\left(\frac{\hat{u} \cdot \tilde{u}}{\sqrt{d}} \right)^{2k} \right] \\ &= \sum_{k=0}^D \frac{(\beta^k (2k-1)!!)^2}{(2k)! \gamma^k} = \sum_{k=0}^D \frac{(2k-1)!!}{(2k)!} \frac{\beta^{2k}}{\gamma^k} \end{aligned} \quad (\text{B.23})$$

which is what we wanted to prove.

As a final note we remark that the basic ideas of the arguments in [57] coincide with what exposed above. However, the increased generality of the statement requires the use of the abstract theory of Umbral calculus to generalize the notion of Hermite polynomials to negative SNR cases, as well as more technical work to achieve the bounds on the LDLR projections.

B.3 Details on the spiked cumulant model

Here we will expand on the mathematical details of the spiked cumulant model of section 3.1.

B.3.1 Prior distribution on the spike

For the prior distribution on u , \mathcal{P} , its role is analogous to the spiked Wishart model, so all the choices commonly used for that model can be considered applicable to this case. Namely symmetric distributions so that $\|\frac{u}{\sqrt{d}}\| \approx 1$ as $d \rightarrow \infty$. In the following we will make the computations assuming u_i i.i.d. and with Rademacher prior:

$$u_i \sim \text{Rademacher}(1/2) \quad (\text{B.24})$$

It helps to have i.i.d. components and constant norm $\|\frac{u}{\sqrt{d}}\| \equiv 1$. However all the results should hold, with more involved computations, also with the following priors:

- $(u_i)_{i=1, \dots, d}$ are i.i.d. and $u_i \sim \mathcal{N}(0, 1)$
- $u \in \text{Unif}(\partial B(0, \sqrt{d}))$.

B.3.2 Distribution of the non-Gaussianity

As detailed in assumption 3.1, we need the non-Gaussianity to satisfy specific conditions. Some of the requirements are fundamental and cannot be avoided, whereas others could likely be removed or modified with only technical repercussion that do not change the essence of the results.

The most vital assumptions are the first and the last: $\mathbb{E}[g] \neq 0$ would introduce signal in the first cumulant, changing completely the model. It is important to control the tails of the distribution with

$$\mathbb{E}[\exp(g^2/2)] < +\infty, \quad (\text{B.25})$$

a fat-tailed g would make the LR-LDLR technique pointless due to the fact that $L \notin \mathcal{L}^2(\mathbb{R}^d, \mathbb{Q})$ and $\|L\| = \infty$ for any n, d . For example it is not possible to use Laplace distribution for g .

On the opposite side, the least important assumptions are that $\text{Var}(g) = 1$ and eq. (10); removing the first would just change the formula for whitening matrix S , while eq. (10) is a very weak requirement and it is needed just to estimate easily the Hermite coefficients contribution and reach eq. (16), it may be even possible to remove it and try to derive a similar estimate from the assumption on the tails eq. (B.25).

Finally, the requirement of symmetry of the distribution has been chosen arbitrarily thinking about applications: the idea is that the magnitude of the fourth order cumulant, the kurtosis, is sometimes used as a test for non-Gaussianity, so it is interesting to isolate the contribution given by the kurtosis, and higher order, even degree, cumulants, by cancelling the contribution of odd order cumulants. However, it would be interesting to extend the model in the case of a centered distribution with non zero third order cumulant. It is likely that the same techniques can be applied, but the final thresholds on θ may differ.

The following lemma gives a criterion of admissibility that ensures Radem(1/2) and Unif($-\sqrt{3}, \sqrt{3}$) (together with many other compactly supported distributions) satisfy assumption 3.1.

Lemma B.4. *Suppose p_g is a probability distribution, compactly supported in $[-\Lambda, \Lambda]$, $\Lambda \geq 1$, then*

$$\mathbb{E}_{g \sim p_g} [h_m(g)] \leq \Lambda^m m!$$

Proof. Use the notation $h_m(x) = \sum_{k=0}^m a_{m,k} x^k$ and $S_m := \sum_{k=0}^m |a_{m,k}|$. Then we have that

$$\begin{aligned} \mathbb{E}_{g \sim p_g} [h_m(g)] &= \mathbb{E}_{g \sim p_g} \left[\sum_{k=0}^m a_{m,k} g^k \right] \\ &\leq \mathbb{E}_{g \sim p_g} \left[\sum_{k=0}^m |a_{m,k}| |g|^k \right] \\ &\leq \Lambda^m S_m \end{aligned} \quad (\text{B.26})$$

So we just need to prove that $S_m \leq m!$, which can be done by induction using eq. (B.8). Suppose it true for m , we prove it for $m+1$. By eq. (B.8) we have that:

$$|a_{m+1,k}| \leq \begin{cases} |a_{m,1}| & k=0 \\ |a_{m,k-1}| + (k+1)|a_{m,k+1}| & k>0 \end{cases} \quad (\text{B.27})$$

Summing on both sides (and using $a_{m,k} = 0$ when $k > m$), we get:

$$\begin{aligned} S_{m+1} &\leq |a_{m,1}| + \sum_{k=1}^{m+1} |a_{m,k-1}| + (k+1)|a_{m,k+1}| \\ S_{m+1} &\leq S_m + \sum_{j=0}^m j|a_{m,j}| \\ S_{m+1} &\leq S_m + m \sum_{j=0}^m |a_{m,j}| \\ S_{m+1} &\leq (m+1)S_m \end{aligned} \quad (\text{B.28})$$

Hence by application of the inductive hypothesis we get $S_{m+1} \leq (m+1)!$, completing the proof. \square

B.3.3 Computing the whitening matrix

In this paragraph all the expectations are made assuming u fixed and it will be best to work with its normalized version $\bar{u} = u/\sqrt{d}$. Note that $\mathbb{E}[x] = 0$ and we want also that

$$\begin{aligned} \mathbb{1}_{d \times d} &= \mathbb{E}[xx^\top] = \mathbb{E}[S(\sqrt{\beta}g\bar{u} + z)(\sqrt{\beta}g\bar{u}^\top + z^\top)S^\top] \\ &= S(\mathbb{1} + \beta\bar{u}\bar{u}^\top)S^\top \end{aligned} \quad (\text{B.29})$$

Hence we need

$$S^2 = SS^\top = (\mathbb{1} + \beta\bar{u}\bar{u}^\top)^{-1} = \mathbb{1} - \frac{\beta}{1+\beta}\bar{u}\bar{u}^\top \quad (\text{B.30})$$

So we look for γ such that:

$$(\mathbb{1} + \gamma\bar{u}\bar{u}^\top)^2 = \mathbb{1} - \frac{\beta}{1+\beta}\bar{u}\bar{u}^\top \quad (\text{B.31})$$

By solving the second order equation we get

$$\gamma_\pm = -\left(1 \pm \frac{1}{\sqrt{1+\beta}}\right) \quad (\text{B.32})$$

We choose the solution with $-$, so that S is positive definite:

$$S = \mathbb{1} - \left(1 - \frac{1}{\sqrt{1+\beta}}\right)\bar{u}\bar{u}^\top = \mathbb{1} - \frac{\beta}{1+\beta+\sqrt{1+\beta}}\frac{uu^\top}{d}. \quad (\text{B.33})$$

Hence we can compute also the explicit expression for x :

$$\begin{aligned} x &= z - \left(1 - \frac{1}{\sqrt{1+\beta}}\right)\bar{u}^\top z \bar{u} + \sqrt{\frac{\beta}{1+\beta}}g\bar{u} \\ x &= \underbrace{z - \bar{u}^\top z \bar{u}}_{z_{\perp u}} + \left(\sqrt{\frac{1}{1+\beta}}\bar{u}^\top z + \underbrace{\sqrt{\frac{\beta}{1+\beta}}g}_{\eta} \right) \bar{u} \\ &= z_{\perp u} + \left(\sqrt{1 - \eta^2}\bar{u}^\top z + \eta g \right) \bar{u} \end{aligned} \quad (\text{B.34})$$

So x is standard Gaussian in the directions orthogonal to u , whereas in u direction, it is a weighted sum between g and z . Note that it is a quadratic interpolation: the sum of the square of the weights is 1.

B.4 Details of the LR analysis for spiked cumulant model

B.4.1 Proof sketch for theorem 3.2

Since the samples are independent, the total LR factorises as

$$L(\underline{y}) = \mathbb{E}_u \left[\prod_{\mu=1}^n l(y^\mu | u) \right], \quad (\text{B.35})$$

where the sample-wise likelihood ratio

$$l(y|u) = \frac{p_x(y|u)}{p_z(y)} = \mathbb{E}_{g \sim p_g} \left[\sqrt{1+\beta} \exp \left(-\frac{1+\beta}{2} \left(g - \sqrt{\frac{\beta}{(1+\beta)d}} y \cdot u \right)^2 + \frac{g^2}{2} \right) \right]. \quad (\text{B.36})$$

To compute the norm of the LR, we consider two independent replicas of the spike, u and v , to get

$$\|L_{n,d}\|^2 = \mathbb{E}_{\underline{y} \sim \underline{\mathbb{Q}}} \left[\mathbb{E}_u \left[\prod_{\mu=1}^n l(y^\mu | u) \right] \mathbb{E}_v \left[\prod_{\mu=1}^n l(y^\mu | v) \right] \right]. \quad (\text{B.37})$$

The hard part now is to simplify the high-dimensional integrals in this expression, it can be done because the integrand is almost completely symmetric, and the only asymmetries lie on the subspace spanned by u and v .

$$\|L_{n,d}\|^2 = \mathbb{E}_{u,v} \left[\mathbb{E}_{g_u, g_v} \left[\frac{1 + \beta}{\sqrt{(1 + \beta)^2 - \beta^2 \left(\frac{u \cdot v}{d}\right)^2}} e^{-\frac{(1 + \beta)((1 + \beta)(g_u^2 + g_v^2) - 2\beta(g_u g_v)(\frac{u \cdot v}{d}))}{2(1 + \beta)^2 - 2\beta^2 \left(\frac{u \cdot v}{d}\right)^2} + \frac{g_u^2 + g_v^2}{2}} \right] \right]^n$$

Note that the integrand depends on u and v only through $\frac{u \cdot v}{d} =: \lambda$. So, using that the prior on u, v is i.i.d. Rademacher, the outer expectation can be transformed in a one dimensional expectation over λ , leading to (11).

B.4.2 Proof of theorem 3.2

$\tilde{x}^\mu = \sqrt{\frac{\beta}{d}} g^\mu u + z^\mu$, to find the marginal density of x^μ we integrate over the possible values of g

$$p_{\tilde{x}}(y|u) = \mathbb{P}(\tilde{x}^\mu \in dy|u) = \mathbb{E}_g \left[p_z \left(y - \sqrt{\frac{\beta}{d}} g u \right) \right] \quad (\text{B.38})$$

where p_z is the density of a standard normal d -dimensional variable $z \sim \mathcal{N}(0, \mathbb{1}_d)$. But we are interested in the density of the whitened variable x , $p_x(\cdot|u)$, which can be seen as the push forward of the density of \tilde{x} with respect to the linear transformation S . So

$$p_x(y|u) = p_{\tilde{x}}(S^{-1}y|u) |\det S^{-1}|. \quad (\text{B.39})$$

It is easy to see from eq. (9) that $|\det S^{-1}| = \sqrt{1 + \beta}$, so we can plug it into eq. (B.38) and after expanding the computations we get to

$$p_x(y|u) = p_z(y) \mathbb{E}_g \left[\sqrt{1 + \beta} \exp \left(-\frac{1 + \beta}{2} \left(g - \sqrt{\frac{\beta}{(1 + \beta)d}} y \cdot u \right)^2 + \frac{g^2}{2} \right) \right]. \quad (\text{B.40})$$

So we have found the likelihood ratio for a single sample, conditioned on the spike:

$$l(y|u) = \frac{p_x(y|u)}{p_z(y)} = \mathbb{E}_g \left[\sqrt{1 + \beta} \exp \left(-\frac{1 + \beta}{2} \left(g - \sqrt{\frac{\beta}{(1 + \beta)d}} y \cdot u \right)^2 + \frac{g^2}{2} \right) \right]. \quad (\text{B.41})$$

Note that conditioning on u the samples are independent, so we have the following formula:

$$L(\underline{y}) = \mathbb{E}_u \left[\prod_{\mu=1}^n l(y^\mu | u) \right]. \quad (\text{B.42})$$

So to compute the norm we consider two independent replicas of the spike, u and v , then we switch the

order of integration to get

$$\begin{aligned}
||L_{n,d}||^2 &= \mathbb{E}_{\underline{y} \sim \mathbb{Q}} \left[\mathbb{E}_u \left[\prod_{\mu=1}^n l(y^\mu | u) \right] \mathbb{E}_v \left[\prod_{\mu=1}^n l(y^\mu | v) \right] \right] \\
&= \mathbb{E}_{u,v} \left[\mathbb{E}_{\underline{y} \sim \mathbb{Q}} \left[\prod_{\mu=1}^n l(y^\mu | u) l(y^\mu | v) \right] \right] \\
&= \mathbb{E}_{u,v} \left[\mathbb{E}_{\underline{y} \sim \mathbb{Q}} [l(y|u)l(y|v)]^n \right] \tag{B.43} \\
&= \mathbb{E}_{u,v} \left[\mathbb{E}_{\underline{y} \sim \mathbb{Q}} \left(\mathbb{E}_{g_u} \left[\sqrt{1+\beta} \exp \left(-\frac{1+\beta}{2} \left(g_u - \sqrt{\frac{\beta}{(1+\beta)d}} y \cdot u \right)^2 + \frac{g_u^2}{2} \right) \right] \right. \right. \\
&\quad \left. \left. \cdot \mathbb{E}_{g_v} \left[\sqrt{1+\beta} \exp \left(-\frac{1+\beta}{2} \left(g_v - \sqrt{\frac{\beta}{(1+\beta)d}} y \cdot v \right)^2 + \frac{g_v^2}{2} \right) \right] \right) \right]^n \right].
\end{aligned}$$

Switching the integral over y inside the new integrals over g_u and g_v we can isolate the following integral over y :

$$I := \mathbb{E}_{\underline{y} \sim \mathbb{Q}} \left[\exp \left(-\frac{1+\beta}{2} \left(g_u - \sqrt{\frac{\beta}{(1+\beta)d}} y \cdot u \right)^2 - \frac{1+\beta}{2} \left(g_v - \sqrt{\frac{\beta}{(1+\beta)d}} y \cdot v \right)^2 \right) \right]. \tag{B.44}$$

It can be computed by noting the subspace orthogonal to $\{u, v\}$, we just have the integral of a standard normal, and the remaining 2 dimensional integral can be computed explicitly. Since the Rademacher prior implies that $||u|| = ||v|| = \sqrt{d}$, the result depends only on their overlap λ (i.e. $\lambda = \frac{u \cdot v}{d}$), leading to:

$$I = \frac{1}{\sqrt{(1+\beta)^2 - \beta^2 \lambda^2}} \exp \left(-\frac{1+\beta}{2(1+\beta)^2 - 2\beta^2 \lambda^2} ((1+\beta)(g_u^2 + g_v^2) - 2\beta(g_u g_v) \lambda) \right) \tag{B.45}$$

If we plug this formula inside eq. (B.43) and rearrange the terms we get an expression that can be written in terms of the density of two bi-dimensional centered Gaussians

$$\begin{aligned}
||L_{n,d}||^2 &= \mathbb{E}_{\lambda} \left[\mathbb{E}_{g_u, g_v} \left[\frac{1+\beta}{\sqrt{(1+\beta)^2 - \beta^2 \lambda^2}} e^{-\frac{(1+\beta)((1+\beta)(g_u^2 + g_v^2) - 2\beta(g_u g_v) \lambda)}{2(1+\beta)^2 - 2\beta^2 \lambda^2} + \frac{g_u^2 + g_v^2}{2}} \right]^n \right] \\
&= \mathbb{E}_{\lambda} \left[\mathbb{E}_{g_u, g_v} \left[\mathcal{N}((g_u, g_v); \Sigma) \mathcal{N}((g_u, g_v); \mathbb{1}_{2 \times 2})^{-1} \right]^n \right].
\end{aligned} \tag{B.46}$$

Where

$$\Sigma^{-1} = \frac{1+\beta}{(1+\beta)^2 - \beta^2 \lambda^2} \begin{pmatrix} 1+\beta & -\beta \lambda \\ -\beta \lambda & 1+\beta \end{pmatrix}, \quad \lambda = \frac{u \cdot v}{d}. \tag{B.47}$$

Now we turn to compute the expectation over λ . Note that since u, v are independent and their components are Rademacher distributed, product of Rademacher is still Rademacher, hence $u \cdot v$ is the sum of d independent Rademacher random variables. Using moreover that the Rademacher distribution is just a linear transformation of the Bernoulli, we can link the distribution of the overlap λ to a linear transformation of a binomial distribution: $\frac{d}{2}(\lambda + 1) \sim \text{Binom}(d, 1/2)$.

We therefore define the auxiliary function

$$f(\beta, \lambda) := \mathbb{E}_{g_u, g_v} \left[\frac{1+\beta}{\sqrt{(1+\beta)^2 - \beta^2 \lambda^2}} e^{-\frac{(1+\beta)((1+\beta)(g_u^2 + g_v^2) - 2\beta(g_u g_v) \lambda)}{2(1+\beta)^2 - 2\beta^2 \lambda^2} + \frac{g_u^2 + g_v^2}{2}} \right] \tag{B.48}$$

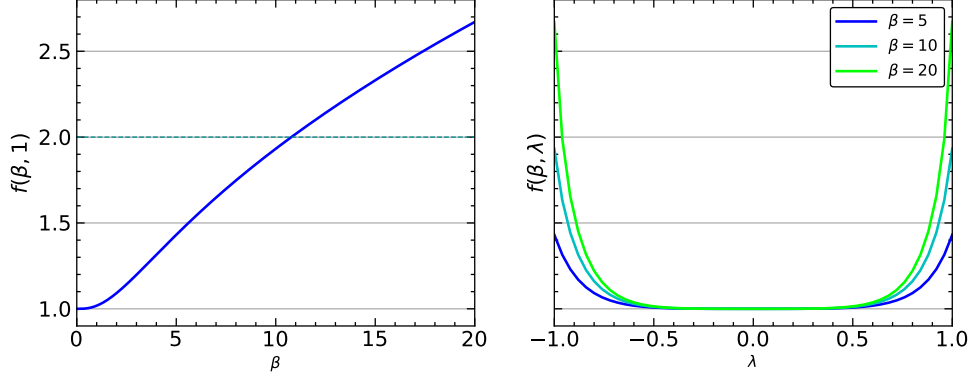


Figure B.1: Graphs of f , defined in (B.48), when $g \sim \text{Rademacher}(1/2)$.

so that the LR norm can be rewritten as

$$\|L_{n,d}\|^2 = \sum_{j=0}^d \binom{d}{j} \frac{1}{2^d} f\left(\beta, \frac{2j}{d} - 1\right)^n \quad (\text{B.49})$$

which is what we needed to prove.

B.4.3 Rademacher non Gaussianity

The precise value of f depends on the choice of distribution for the non Gaussianity g . We will analyze in more detail the case in which $g \sim \text{Rademacher}(1/2)$. It is a case that is particularly interesting for the point of view of the applications because it amounts to comparing a standard Gaussian with a Gaussian mixture with same mean and covariance. Moreover, with this choice of non Gaussianity, the technical work simplifies because the troublesome integral over g_u, g_v in eq. (B.48) becomes just a simple sum over 4 possibilities. In this case f can be computed exactly and it is displayed in fig. B.1. The maximum of $f(\beta, \cdot)$ is attained at $\lambda = \pm 1$ and $f(\cdot, 1)$ is monotonically increasing. Assume that $n \asymp d^\theta$, then a sufficient condition for LR to diverge is $\frac{f(\beta, 1)^{d^\theta}}{2^d} \rightarrow \infty$, which holds as soon as $\theta > 1$. Moreover, even at linear sample complexity, it is possible to find regimes that ensure divergence of the LR norm, similar to BBP phase transition in spiked Wishart model. Assume that samples and dimensions scale at the same rate as in spiked Wishart model: $n \asymp \frac{d}{\gamma}$, then a sufficient condition for divergence is that

$$\frac{f(\beta, 1)^{d/\gamma}}{2^d} \rightarrow \infty$$

which holds if and only if $f(\beta, 1)^{1/\gamma} > 2$. Hence given β , you can always find

$$\gamma_\beta := \frac{\log(f(\beta, 1))}{\log 2} \quad (\text{B.50})$$

And for $\gamma > \gamma_\beta$ there is guarantee that $\|L_{n,d}\| \rightarrow \infty$. Vice-versa, we could also fix γ and define β_γ as only value of β that makes eq. (B.50) true.

It is spontaneous to ask whether this condition for divergence of LR norm is also necessary, making the SNR threshold β_γ the analogous in this model of the threshold $\beta_c = \sqrt{\gamma}$ in spiked Wishart model (theorem 2.4). Although a rigorous proof of this is still missing, numerical evidence (fig. B.2) suggests that for $\beta \leq \beta_\gamma$ the LR norm stays indeed bounded. Of course, this would extend to $\theta < 1$, since $\|L\|$ is monotonically increasing in θ .

B.5 Proofs for LDLR on spiked cumulant model

Here we present the proofs of theorem 3.3 and corollary 3.4. We first give a sketch of the proof in appendix B.5.1 before giving the detailed proof in appendix B.5.2.

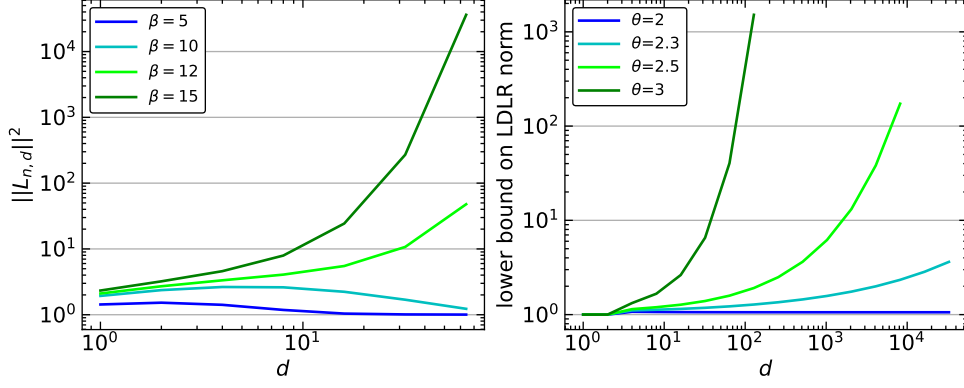


Figure B.2: On the left, LR norm when $g \sim \text{Rademacher}(1/2)$ in the regime $n = \gamma d$ with $\gamma = 1$. When $\beta < \beta_\gamma \approx 10.7$ the likelihood ratio remains bounded, whereas it goes to $+\infty$ for $\beta > \beta_\gamma$. On the right, the lower bound on $\|L_{n,d}^{\leq D(n)}\|$ given by eq. (13) goes to $+\infty$ for $\theta > 2$. Parameters for the plot: $g \sim \text{Radem}(1/2)$, $\beta = 10$, $D(n) = \log^{3/2}(n)$

B.5.1 Proof sketch

The starting point of the argument is the observation that since the null hypothesis is white Gaussian noise, the space $L^2(\mathbb{R}^{nd}, \langle \cdot, \cdot \rangle)$ has an explicit orthogonal basis in the set of multivariate Hermite polynomials (H_α). The multi-index $\alpha \in \mathbb{N}^{nd}$ denotes the degree of the Hermite polynomial which is computed for each entry of the data matrix; see appendix B.1.2 for a detailed explanation. We can then expand the LDLR norm in this basis to write:

$$\|L_{n,d}^{\leq D}\|^2 = \sum_{|\alpha| \leq D} \frac{\langle L, H_\alpha \rangle^2}{\alpha!} = \sum_{|\alpha| \leq D} \frac{1}{\alpha!} \mathbb{E}_{x \sim \mathbb{P}} [H_\alpha(x)]^2 \quad (\text{B.51})$$

From now on the two bounds are treated separately.

Lower bound The idea is to bound the LDLR from below by computing the sum eq. (B.51) only over a restricted set of addends \mathcal{I}_m which we can compute explicitly. In particular, we consider the set \mathcal{I}_m of all the polynomials with degree $4m$ in the data matrix, which are at most of order 4 in each individual sample x^μ . Then we use that the expectation of such Hermite polynomials conditioned on u can be split into m integrals of degree-4 Hermite polynomials in d variables. In this way we can use our knowledge of the fourth-order cumulant of x to compute those expectations (see eq. (B.69)), so we find that

$$\|L_{n,d}^{\leq D}\|^2 \geq \sum_m \sum_{|\alpha| \in \mathcal{I}_m} \frac{1}{\alpha!} \mathbb{E}_{x \sim \mathbb{P}} [H_\alpha(x)]^2 \geq \sum_m \sum_{\alpha \in \mathcal{I}_m} \left(\frac{\beta^2 \kappa_4^g}{\sqrt{4!} d^2 (1 + \beta)^2} \right)^{2m}. \quad (\text{B.52})$$

Thanks to this manipulation, the bound does not depend on α explicitly, so we can complete the bound by estimating the cardinality of \mathcal{I}_m . Thanks to the fact that we have n i.i.d. copies of variable x at disposal, the class of polynomials \mathcal{I}_m has size that grows at least as $\binom{n}{m} \binom{d+1}{2}^m$, allowing to reach the lower bound in the statement.

Upper bound We can show that the expectation of Hermite polynomials for a single sample x^μ over the distribution $\mathbb{P}(\cdot|u)$ can be written as $\mathbb{E}_{x \sim \mathbb{P}(\cdot|u)} [H_\alpha(x)] = T_{|\alpha|,g} / d^{|\alpha|/2} u^\alpha$, where $T_{|\alpha|,g} = \left(\frac{\beta}{1+\beta} \right)^{|\alpha|/2} \mathbb{E} [h_{|\alpha|}(g)]$, cf. lemma B.5. Using the fact that inputs are sampled i.i.d. from $\mathbb{P}(\cdot|u)$ and substituting this result into eq. (B.51), we find that

$$\|L_{n,d}^{\leq D}\|^2 = \sum_{|\alpha| \leq D} \frac{\left(\prod_{\mu=1}^n T_{|\alpha|^\mu, g} \right)^2}{\alpha! d^{|\alpha|}} \mathbb{E}_{u \sim \mathcal{P}(u)} [u^\alpha]^2. \quad (\text{B.53})$$

To obtain an upper bound, we will first show that many addends in this sum are equal to zero, then estimate the remainder.

On the one hand, since we chose a Rademacher prior over the elements of the spike u_i , the expectation over the prior yields either 1 or 0 depending on whether the exponent of each u_i is even or odd. On the other hand, the whitening of the data means that $T_{|\alpha|,g} = 0$ for $0 < |\alpha| < 4$ (as proved in lemma B.5).

For each $m \in \mathbb{N}$, we can denote \mathcal{A}_m the set of multi-indices $|\underline{\alpha}| = m$ that give non-zero contributions in eq. (B.53), so that we can write:

$$\|L_{n,d}^{\leq D}\|^2 = \sum_{m=0}^D \sum_{\underline{\alpha} \in \mathcal{A}_m} \frac{\left(\prod_{\mu=1}^n T_{|\alpha^\mu|,g}\right)^2}{\underline{\alpha}! d^m} \quad (\text{B.54})$$

Now we proved that we can bound the inner terms so that they depend on $\underline{\alpha}$ only through the norm $|\underline{\alpha}| = m$ (cf. eq. (B.58) and eq. (B.86)):

$$\begin{aligned} \|L_{n,d}^{\leq D}\|^2 &\leq \sum_{m=0}^D \sum_{\underline{\alpha} \in \mathcal{A}_m} \frac{1}{d^m} \left(\frac{\beta}{1+\beta}\right)^m \sup_{k \leq m} \left(\mathbb{E}[h_k(g)]^{2m/k}\right) \\ &= \sum_{m=0}^D \frac{1}{d^m} \left(\frac{\beta}{1+\beta}\right)^m \sup_{k \leq m} \left(\mathbb{E}[h_k(g)]^{2m/k}\right) \#\mathcal{A}_m \end{aligned} \quad (\text{B.55})$$

Finally, the cardinality of \mathcal{A}_m is 1 in case $m = 0$ (which leads to the addend 1 in eq. (14)) and if $m > 0$ it can be bounded by (for details see eq. (B.87) in the appendix)

$$\binom{\lfloor m/4 \rfloor \lfloor m/2 \rfloor + m - 1}{m} \binom{n}{\lfloor m/4 \rfloor} \binom{d}{\lfloor m/2 \rfloor}, \quad (\text{B.56})$$

leading to (14).

B.5.2 Detailed proof

First we prove a lemma that provides formulas and estimates for projections of the sample-wise likelihood ratio $l(\cdot|u)$ on the Hermite polynomials.

Lemma B.5. *Let $x = S\left(\sqrt{\beta/d}gu + z\right)$ be a spiked cumulant random variable. Then for any $\alpha \in \mathbb{N}^d$, with $|\alpha| = m$, we have that:*

$$\langle l(\cdot|u), H_\alpha \rangle = \mathbb{E}_{x \sim \mathbb{P}(\cdot|u)} [H_\alpha(x)] = \frac{T_{m,g}}{d^{m/2}} u^\alpha \quad (\text{B.57})$$

where $T_{m,g}$ is a coefficient defined as:

$$T_{m,g} = \left(\frac{\beta}{1+\beta}\right)^{m/2} \mathbb{E}[h_m(g)] \quad (\text{B.58})$$

Proof. Recall that by (B.36)

$$l(y|u) = \mathbb{E}_g \left[\sqrt{1+\beta} \exp \left(-\frac{1}{2} \left(\sqrt{1+\beta}g - \sqrt{\frac{\beta}{d}}y \cdot u \right)^2 + \frac{g^2}{2} \right) \right]. \quad (\text{B.59})$$

Note that this expression, thanks to eq. (B.25) that bounds the integral, is differentiable infinitely many times in the y variable. It can be quickly proven by induction on $|\alpha| = m$ (using the recursive definition

of Hermite polynomials eq. (B.7)) that:

$$\partial_{\alpha} l(y|u) = \left(\frac{\beta}{d}\right)^{m/2} u^{\alpha} \cdot \mathbb{E}_g \left[\sqrt{1+\beta} h_m \left(\sqrt{1+\beta} g - \sqrt{\frac{\beta}{d}} y \cdot u \right) \exp \left(-\frac{1}{2} \left(\sqrt{1+\beta} g - \sqrt{\frac{\beta}{d}} y \cdot u \right)^2 + \frac{g^2}{2} \right) \right] \quad (\text{B.60})$$

Hence we can again use eq. (B.25) together with the fact that

$$\sup_g \left| h_m \left(\sqrt{1+\beta} g - \sqrt{\frac{\beta}{d}} y \cdot u \right) \exp \left(-\frac{1}{2} \left(\sqrt{1+\beta} g - \sqrt{\frac{\beta}{d}} y \cdot u \right)^2 \right) \right| < \infty$$

to deduce that the hypothesis of lemma B.3 are met for any $\alpha \in \mathbb{N}^d$, leading to:

$$\langle l(\cdot|u), H_{\alpha} \rangle = \mathbb{E}_{x \sim \mathbb{P}(\cdot|u)} [H_{\alpha}(x)] = \mathbb{E}_{y \sim \mathbb{Q}} [\partial_{\alpha} l(y|u)] \quad (\text{B.61})$$

This, and eq. (B.60) already prove eq. (B.57). Now to compute the exact value of $T_{m,g}$ we need to take the expectation with respect to $y \sim \mathbb{Q} = \mathcal{N}(0, \mathbb{1}_{d \times d})$. Note that by the choice of Rademacher prior on u , we know that $\|u\| = \sqrt{d}$. So, conditioning on u , $y \cdot \frac{u}{\sqrt{d}} \sim \mathcal{N}(0, 1)$. Hence switching the expectations in eq. (B.60), we get:

$$\begin{aligned} T_{m,g} &= \beta^{m/2} \mathbb{E}_g \left[\int_{-\infty}^{\infty} \frac{dz}{\sqrt{2\pi}} \sqrt{1+\beta} h_m \left(\sqrt{1+\beta} g - \sqrt{\beta} z \right) e^{-\frac{1}{2}(\sqrt{1+\beta} g - \sqrt{\beta} z)^2 + \frac{g^2 - z^2}{2}} \right] \\ &= \beta^{m/2} \mathbb{E}_g \left[\int_{-\infty}^{\infty} \frac{dz}{\sqrt{2\pi}} \sqrt{1+\beta} h_m \left(\sqrt{1+\beta} g - \sqrt{\beta} z \right) \exp \left(-\frac{1}{2} \left(\sqrt{\beta} g - \sqrt{1+\beta} z \right)^2 \right) \right] \\ &\stackrel{\tilde{z} = \sqrt{1+\beta} z}{=} \beta^{m/2} \mathbb{E}_g \left[\int_{-\infty}^{\infty} \frac{d\tilde{z}}{\sqrt{2\pi}} h_m \left(\sqrt{1+\beta} g - \sqrt{\frac{\beta}{1+\beta}} \tilde{z} \right) \exp \left(-\frac{1}{2} \left(\sqrt{\beta} g - \tilde{z} \right)^2 \right) \right] \end{aligned} \quad (\text{B.62})$$

Now we use eq. (B.9) on

$$\begin{aligned} x &= \frac{\beta}{\sqrt{1+\beta}} g - \sqrt{\frac{\beta}{1+\beta}} \tilde{z} \\ y &= \sqrt{1+\beta} g - \frac{\beta}{\sqrt{1+\beta}} g = \frac{g}{\sqrt{1+\beta}} \end{aligned} \quad (\text{B.63})$$

applying also the translation change of variable $\hat{z} = \tilde{z} - \sqrt{\beta} g$ we get:

$$\mathbb{E}_{y \sim \mathbb{Q}} [\partial_{\alpha} l(y|u)] = \left(\frac{\beta}{d}\right)^{m/2} u^{\alpha} \mathbb{E}_g \left[\sum_{k=0}^m \binom{m}{k} h_k \left(\frac{g}{\sqrt{1+\beta}} \right) \left(-\sqrt{\frac{\beta}{1+\beta}} \right)^{m-k} \mathbb{E}_{\hat{z} \sim \mathcal{N}(0,1)} [\hat{z}^{m-k}] \right] \quad (\text{B.64})$$

Now recall the formula for the moments of the standard Gaussian (see for instance section 3.9 in [85]):

$$\mathbb{E}_{\hat{z} \sim \mathcal{N}(0,1)} [\hat{z}^{m-k}] = \begin{cases} (m-k-1)!! & \text{if } m-k \text{ is even} \\ 0 & \text{if } m-k \text{ is odd} \end{cases} \quad (\text{B.65})$$

Plugging this formula inside and changing the summation index $2j := m - k$ we get

$$T_{m,g} = \beta^{m/2} \sum_{j=0}^{\lfloor m/2 \rfloor} \binom{m}{2j} \left(\frac{\beta}{1+\beta} \right)^j (2j-1)!! \mathbb{E} \left[h_{m-2j} \left(\frac{g}{\sqrt{1+\beta}} \right) \right]. \quad (\text{B.66})$$

Note that eq. (B.10) with $x = \frac{g}{\sqrt{1+\beta}}$ and $\gamma = \sqrt{1+\beta}$ gives the following rewriting of $h_m(g)$:

$$h_m(g) = \sum_{j=0}^{\lfloor m/2 \rfloor} (\sqrt{1-\beta})^{m-2j} (\beta)^j \binom{m}{2j} (2j-1)!! h_{m-2j} \left(\frac{g}{\sqrt{1+\beta}} \right) \quad (\text{B.67})$$

which is almost the same expression as in eq. (B.66). This allows simplify everything, leading to eq. (B.58). \square

Note that lemma B.5 together with assumption 3.1 on g imply:

$$m = 2 \text{ or } m \text{ odd} \implies T_{m,g} = 0, \quad (\text{B.68})$$

So, apart from $m = 0$ which gives the trivial contribution +1, the first non zero contributions to the LDLR norm is at degree $m = 4$:

$$\mathbb{E}_{x \sim \mathbb{P}(\cdot|u)} [H_{\alpha}(x)] = \frac{\beta^2}{(1+\beta)^2} \kappa_4^g \frac{u^{\alpha}}{d^2} \quad (\text{B.69})$$

From now on we will consider separately the lower and the upper bounds.

Lower bound The idea of the proof is to start from

$$\|L_{n,d}^{\leq D}\|^2 = \sum_{\substack{\alpha \in \mathbb{N}^{nd} \\ |\alpha| \leq D}} \frac{\langle L, H_{\alpha} \rangle^2}{\alpha!} \quad (\text{B.70})$$

and to estimate it from below by picking only few terms in the sum. So we restrict to particular sets of multi-multi-indices for which we can exploit eq. (B.69). Let $m \in \mathbb{N}$ such that $4m \leq D$, define

$$\mathcal{I}_m = \left\{ \alpha \in (\mathbb{N}^d)^n \mid |\alpha| = 4m, |\alpha^{\mu}| \in \{0, 4\} \forall 1 \leq \mu \leq n \right\} \quad (\text{B.71})$$

\mathcal{I}_m is non empty since $m < n$ and for each $\alpha \in \mathcal{I}_m$ we can enumerate all the indices μ_1, \dots, μ_m such that $\alpha^{\mu_i} \neq 0$.

Now we go on to compute the term $\langle L, H_{\alpha} \rangle$ for $\alpha \in \mathcal{I}_m$:

$$\begin{aligned} \langle L, H_{\alpha} \rangle &= \int_{\mathcal{U}} \mathbb{E}_{x \sim \mathbb{P}(\cdot|u)^{\otimes n}} [H_{\alpha}(x)] d\mathcal{P}(u) \\ &= \int_{\mathcal{U}} \mathbb{E}_{x \sim \mathbb{P}(\cdot|u)^{\otimes n}} \left[\prod_{i=1}^m H_{\alpha^{\mu_i}}(x^{\mu_i}) \right] d\mathcal{P}(u) \end{aligned} \quad (\text{B.72})$$

Since the samples are independent conditionally on u , we can split the inner expectation along the m contributing directions:

$$\langle L, H_{\alpha} \rangle = \int_{\mathcal{U}} \prod_{i=1}^m \mathbb{E}_{x \sim \mathbb{P}(\cdot|u)} [H_{\alpha^{\mu_i}}(x^{\mu_i})] d\mathcal{P}(u) \quad (\text{B.73})$$

Now we need to compute the inner d -dimensional expectation. For that we use that $|\alpha^{\mu_i}| = 4$, so, recalling the notation $\eta = \sqrt{\frac{\beta}{1+\beta}}$, we can apply eq. (B.69) to get for each i

$$\mathbb{E}_{x \sim \mathbb{P}(\cdot|u)} [H_{\alpha^{\mu_i}}(x^{\mu_i})] = \frac{\eta^4}{d^2} \kappa_4^g u^{\alpha^{\mu_i}}. \quad (\text{B.74})$$

So the resulting integral can be written in the following way:

$$\langle L, H_{\underline{\alpha}} \rangle = \left(\frac{\eta^4 \kappa_4^g}{d^2} \right)^m \int_{\mathcal{U}} \prod_{j=1}^d u_j^{\gamma_j} d\mathcal{P}(u) \quad (\text{B.75})$$

where for each $j \in \{1, \dots, d\}$, $\gamma_j := \sum_{\mu} \alpha_j^{\mu}$. So we also have that $\sum_j \gamma_j = 4m$.

Now we take the expectation with respect to $\mathcal{P}(u)$, and use the fact that the components are i.i.d. Rademacher so the result depends on the parity of the γ_j in the following way:

$$\langle L, H_{\underline{\alpha}} \rangle = \begin{cases} \left(\frac{\eta^4 \kappa_4^g}{d^2} \right)^m & \text{if all } (\gamma_j)_{j=1, \dots, d} \text{ are even} \\ 0 & \text{if there is at least one } \gamma_j \text{ which is an odd number} \end{cases} \quad (\text{B.76})$$

Hence, if we restrict to the set:

$$\tilde{\mathcal{I}}_m = \left\{ \underline{\alpha} \in \mathcal{I}_m \mid \forall j \in \{1, \dots, d\} \sum_{\mu=1}^n \alpha_j^{\mu} \text{ is even} \right\} \quad (\text{B.77})$$

We have that all the indices belonging to $\tilde{\mathcal{I}}_m$ give the same contribution:

$$\langle L, H_{\underline{\alpha}} \rangle^2 = \left(\frac{\eta^4}{d^2} \kappa_4^g \right)^{2m} \quad (\text{B.78})$$

Also, note that inside \mathcal{I}_m , $\alpha! \leq (4!)^m$, so get the following estimates

$$\begin{aligned} \|L_{n,d}^{\leq D}\|^2 &= \sum_{|\underline{\alpha}| \leq D} \frac{\langle L, H_{\underline{\alpha}} \rangle^2}{\alpha!} \\ &\geq \sum_{m=0}^{\lfloor D/4 \rfloor} \sum_{\underline{\alpha} \in \tilde{\mathcal{I}}_m} \frac{\langle L, H_{\underline{\alpha}} \rangle^2}{\alpha!} \\ &\geq \sum_{m=0}^{\lfloor D/4 \rfloor} \sum_{\underline{\alpha} \in \tilde{\mathcal{I}}_m} \left(\frac{\eta^4 \kappa_4^g}{\sqrt{4!} d^2} \right)^{2m} \\ &\geq \sum_{m=0}^{\lfloor D/4 \rfloor} \# \tilde{\mathcal{I}}_m \left(\frac{\eta^4 \kappa_4^g}{\sqrt{4!} d^2} \right)^{2m} \end{aligned} \quad (\text{B.79})$$

Now we just need to estimate the cardinality of $\tilde{\mathcal{I}}_m$. A lower bound can be provided by considering

$$\hat{\mathcal{I}}_m = \left\{ \underline{\alpha} \in \mathcal{I}_m \mid \forall \mu \in [n] \forall j \in [d] \alpha_j^{\mu} \text{ is even} \right\} \quad (\text{B.80})$$

Clearly $\hat{\mathcal{I}}_m \subseteq \tilde{\mathcal{I}}_m$ and $\# \hat{\mathcal{I}}_m = \binom{n}{m} \binom{d+1}{2}^m$ because first we can pick the $n - m$ rows of $\underline{\alpha}$ that will be 0 in \mathbb{N}^d , which can be done in $\binom{n}{m}$. Then, for each non-zero row, we need to pick two columns (with repetitions) in which to place a 2 and leave all the other entries as 0, that can be done in $\binom{d+1}{2}^m$ ways.

So plugging the lower bound in the previous estimate, we reach the inequality that we wanted to prove:

$$\|L_{n,d}^{\leq D}\|^2 \geq \sum_{m=0}^{\lfloor D/4 \rfloor} \binom{n}{m} \binom{d+1}{2}^m \left(\frac{\eta^4 \kappa_4^g}{\sqrt{4!} d^2} \right)^{2m} = \sum_{m=0}^{\lfloor D/4 \rfloor} \binom{n}{m} \binom{d+1}{2}^m \left(\frac{\beta^2 \kappa_4^g}{\sqrt{4!} d^2 (1 + \beta)^2} \right)^{2m} \quad (\text{B.81})$$

Upper bound We start from (B.51) using the following rewriting:

$$\begin{aligned}
\|L_{n,d}^{\leq D}\|^2 &= \sum_{|\underline{\alpha}| \leq D} \frac{\langle L, H_{\underline{\alpha}} \rangle^2}{\underline{\alpha}!} \\
&= \sum_{|\underline{\alpha}| \leq D} \frac{\mathbb{E}_{x \sim \mathbb{P}} [H_{\underline{\alpha}}(x)]^2}{\underline{\alpha}!} \\
&= \sum_{|\underline{\alpha}| \leq D} \frac{1}{\underline{\alpha}!} \mathbb{E}_{u \sim \mathcal{P}(u)} \left[\prod_{\mu=1}^n \mathbb{E}_{x^\mu \sim \mathbb{P}(\cdot|u)} [H_{\underline{\alpha}^\mu}(x^\mu)] \right]^2
\end{aligned} \tag{B.82}$$

Now use lemma B.5 and plug in the formulas for the inner expectations.

$$\begin{aligned}
\|L_{n,d}^{\leq D}\|^2 &= \sum_{|\underline{\alpha}| \leq D} \frac{1}{\underline{\alpha}!} \mathbb{E}_{u \sim \mathcal{P}(u)} \left[\prod_{\mu=1}^n \frac{T_{|\underline{\alpha}^\mu|,g}}{d^{|\underline{\alpha}^\mu|/2}} u^{\underline{\alpha}^\mu} \right]^2 \\
&= \sum_{|\underline{\alpha}| \leq D} \frac{\left(\prod_{\mu=1}^n T_{|\underline{\alpha}^\mu|,g} \right)^2}{\underline{\alpha}! d^{|\underline{\alpha}|}} \mathbb{E}_{u \sim \mathcal{P}(u)} [u^{\underline{\alpha}}]^2
\end{aligned} \tag{B.83}$$

Now we use our prior assumption that $u_i \stackrel{\text{i.i.d.}}{\sim} \text{Rad}(1/2)$. Note that odd moments of u_i are equal to 0 and even moments are equal to 1, so (denoting by $\chi_A(\cdot)$ the indicator function of set A):

$$\mathbb{E}_{u \sim \mathcal{P}(u)} [u^{\underline{\alpha}}] = \prod_{i=1}^d \mathbb{E}_{u_i \sim \text{Rademacher}(1/2)} \left[u_i^{\sum_{\mu=1}^n \alpha_i^\mu} \right] = \chi_{\{\sum_{\mu=1}^n \alpha_i^\mu \text{ is even for all } i\}}(\underline{\alpha}) \tag{B.84}$$

Now the key point of the proof: this last formula, together with (B.68), imply that most of the addends in the sum in (B.83) are zero. Set $|\underline{\alpha}| = m$, then the set of multi-indices that could give a non-zero contribution is

$$\mathcal{A}_m = \left\{ \underline{\alpha} \in \mathbb{N}^{n \times d} \mid |\underline{\alpha}| = m, \forall \mu \in [n], \underline{\alpha}^\mu = 0 \text{ or } |\underline{\alpha}^\mu| > 4, \text{ and } \forall i \in [d] \sum_{\mu=1}^n \alpha_i^\mu \text{ is even} \right\} \tag{B.85}$$

Using this fact together with (B.58) we get:

$$\begin{aligned}
\|L_{n,d}^{\leq D}\|^2 &= \sum_{m=0}^D \sum_{\underline{\alpha} \in \mathcal{A}_m} \frac{\left(\prod_{\mu=1}^n T_{|\underline{\alpha}^\mu|,g} \right)^2}{\underline{\alpha}! d^{|\underline{\alpha}|}} \\
&\leq \sum_{m=0}^D \sum_{\underline{\alpha} \in \mathcal{A}_m} \frac{1}{d^m} \prod_{\mu=1}^n \left(\left(\frac{\beta}{1+\beta} \right)^{|\underline{\alpha}^\mu|} \mathbb{E} [h_{|\underline{\alpha}^\mu|}(g)]^2 \right) \\
&\leq \sum_{m=0}^D \sum_{\underline{\alpha} \in \mathcal{A}_m} \frac{1}{d^m} \left(\frac{\beta}{1+\beta} \right)^m \sup_{k \leq m} \left(\mathbb{E} [h_k(g)]^{2m/k} \right) \\
&= \sum_{m=0}^D \frac{1}{d^m} \left(\frac{\beta}{1+\beta} \right)^m \sup_{k \leq m} \left(\mathbb{E} [h_k(g)]^{2m/k} \right) \# \mathcal{A}_m
\end{aligned} \tag{B.86}$$

In the third step we used the following inequality

$$\prod_{\mu} \mathbb{E} [h_{|\underline{\alpha}^\mu|}(g)]^2 \leq \prod_{\mu} \sup_{k \leq m} \left(\mathbb{E} [h_k(g)]^{1/k} \right)^{2|\underline{\alpha}^\mu|} = \sup_{k \leq m} \mathbb{E} [h_k(g)]^{2m/k}$$

That holds since $\alpha \in \mathcal{A}_m$ hence $\sum_{\mu} |\alpha^{\mu}| = m$.

It is hard to compute exactly the cardinality of \mathcal{A}_m , but we can estimate it by considering the inclusion $\mathcal{A}_m \subseteq \tilde{\mathcal{A}}_m$ defined as

$$\tilde{\mathcal{A}}_m = \left\{ \alpha \in \mathbb{N}^{n \times d} \mid |\alpha| = m, \text{ there are at most } \left\lfloor \frac{m}{4} \right\rfloor \text{ non-zero rows and } \left\lfloor \frac{m}{2} \right\rfloor \text{ non-zero columns} \right\} \quad (\text{B.87})$$

Assume now $m > 0$ (the case $m = 0$ can be treated separately, leading to the addend +1 in (14)). To compute the cardinality of $\tilde{\mathcal{A}}_m$ we just have to multiply the different contributions

- There are $\binom{n}{\lfloor m/4 \rfloor}$ possibilities for the non-zero rows
- There are $\binom{d}{\lfloor m/2 \rfloor}$ possibilities for the non-zero columns
- once restricted to a $\lfloor m/4 \rfloor \times \lfloor m/2 \rfloor$ we have to place the units to get to norm m . It is the counting problem of placing m units inside the $\lfloor m/4 \rfloor \lfloor m/2 \rfloor$ matrix entries. The possibilities are

$$\binom{\lfloor m/4 \rfloor \lfloor m/2 \rfloor + m - 1}{m} \quad (\text{B.88})$$

So we get the following estimate for the cardinality of \mathcal{A}_m

$$\#\mathcal{A}_m \leq \binom{n}{\lfloor m/4 \rfloor} \binom{d}{\lfloor m/2 \rfloor} \binom{\lfloor m/4 \rfloor \lfloor m/2 \rfloor + m - 1}{m} \quad (\text{B.89})$$

Plugging into (B.86) we reach the final formula (14), which completes the proof.

Proof of corollary 3.4 Now we turn to the proof of corollary 3.4 on the asymptotic behavior of the bound

$$\binom{n}{m} = \frac{n^m}{m!} + O(n^{m-1}) \quad (\text{B.90})$$

$$\binom{d+1}{2}^m \geq \frac{d^{2m}}{2^m} \quad (\text{B.91})$$

So we have that:

$$\begin{aligned} \|L_{n,d}^{\leq D(n)}\|^2 &\geq \sum_{m=0}^{\lfloor D/4 \rfloor} \left(\frac{n^m}{m!} + O(n^{m-1}) \right) \left(\frac{d^{2m}}{2^m} + O(1) \right) \left(\frac{\beta^2 \kappa_4^g}{\sqrt{4!} d^2 (1+\beta)^2} \right)^{2m} \\ &= \left(\sum_{m=0}^{\lfloor D/4 \rfloor} \frac{1}{m!} \left(\frac{\beta^2 \kappa_4^g}{\sqrt{2} \sqrt{4!} (1+\beta)^2} \right)^{2m} \left(\frac{n}{d^2} \right)^m \right) + O \left(\sum_m \frac{n^{m-1}}{m! d^{2m}} \left(\frac{\beta^2 \kappa_4^g}{\sqrt{2} \sqrt{4!} (1+\beta)^2} \right)^{2m} \right) \end{aligned} \quad (\text{B.92})$$

Then we lower-bound the sum by considering just the last term.

$$\|L_{n,d}^{\leq D(n)}\|^2 \geq \frac{1}{\lfloor D/4 \rfloor!} \left(\frac{\beta^2 \kappa_4^g}{\sqrt{2} \sqrt{4!} (1+\beta)^2} \right)^{2\lfloor D/4 \rfloor} \left(\frac{n}{d^2} \right)^{\lfloor D/4 \rfloor} + o \left(\frac{1}{\lfloor D/4 \rfloor!} \left(\frac{Cn}{d^2} \right)^{\lfloor D/4 \rfloor} \right) \quad (\text{B.93})$$

So by using $k! \leq k^k$ on $\lfloor D/4 \rfloor$ and picking n, d large enough so that numerical constants and the $o(\dots)$ become negligible for the estimate, we get (15).

Plugging in the scaling $n \asymp d^{\theta}$ and $D(n) \asymp \log^{1+\varepsilon}(n)$ it is clear that what decides the behaviour of the sequence is the term $\frac{n}{d^2}$.

- If $0 < \theta \leq 2$, $\frac{n}{d^2} \rightarrow 0$ and so (15) does not provide information on the divergence of the LDLR norm.

- if $\theta > 2$ it is $\frac{n}{d^2} \rightarrow \infty$ faster than the logarithmic term at denominator, so the right hand side in (15) diverges at ∞ , proving the second regime in (17)

Now let us turn to proving (16). We are in the regime $m \leq D \ll \min(n, d)$, hence we can use the following estimates of binomial coefficients and factorial

$$\begin{aligned} \binom{n}{\lfloor m/4 \rfloor} &\leq n^{m/4} \\ \binom{d}{\lfloor m/2 \rfloor} &\leq d^{m/2} \\ \binom{\lfloor m/4 \rfloor \lfloor m/2 \rfloor + m - 1}{m} &\leq (m^2/8)^m \\ m! &\leq m^m \end{aligned} \quad (\text{B.94})$$

on eq. (14) to get

$$\|L_{n,d}^{\leq D}\|^2 \leq 1 + \sum_{m=1}^D \left(\frac{\beta}{1+\beta} \right)^m m^{2m} \sup_{k \leq m} \left(\mathbb{E}[h_k(g)]^{2m/k} \right) \left(\frac{n}{d^2} \right)^{m/4} \quad (\text{B.95})$$

Now we use estimate the term depending on the Hermite coefficients of g , using the assumption eq. (10):

$$\begin{aligned} \sup_{k \leq m} \left(\mathbb{E}[h_k(g)]^{2m/k} \right) &\leq \sup_{k \leq m} \left((\Lambda^k k!)^{2m/k} \right) \\ &\leq \Lambda^{2m} \sup_{k \leq m} (k^{2m}) \\ &\leq \Lambda^{2m} m^{2m} \end{aligned} \quad (\text{B.96})$$

Plugging into the estimate for the LDLR we get (16)

$$\|L_{n,d}^{\leq D}\|^2 \leq 1 + \sum_{m=1}^D \left(\frac{\Lambda^2 \beta}{1+\beta} \right)^m m^{4m} \left(\frac{n}{d^2} \right)^{m/4} \quad (\text{B.97})$$

By letting $n \asymp d^\theta$, for $\theta > 0$ and $D(n) \asymp \log^{1+\varepsilon}(n)$, we can see that the bound goes to 1 when $\theta < 2$, proving the first regime in (17).

C Details on the replica analysis

We analytically compute the generalisation error of a random feature model trained on the Gaussian mixture classification task of section 2 by exploiting the Gaussian equivalence theorem for dealing with structured data distributions [66–70]. In particular, we use equations derived by Loureiro *et al.* [65] that describe the generalisation error of random features on Gaussian mixture classification using the replica method of statistical physics. The equations describe the high-dimensional limit where n, d , and the size of the hidden layer $p \rightarrow \infty$ while their ratios stay finite, $\alpha = n/d$ and $\gamma = d/p \sim O(1)$. In this regime, the generalisation error is a function of only scalar quantities, i.e.

$$\epsilon_g = 1 - \rho_+ \mathbb{E}_\xi \left[\text{sign} \left(m_+^* + \sqrt{q_+^*} \xi + b^* \right) \right] + \rho_- \mathbb{E}_\xi \left[\text{sign} \left(m_-^* + \sqrt{q_-^*} \xi + b^* \right) \right], \quad (\text{C.1})$$

where $\xi \sim \mathcal{N}(0, 1)$, ρ_\pm defines the fraction of data point belonging to class $y = \pm 1$ while m_\pm^* , q_\pm^* and b^* are the so-called overlap parameters and bias term respectively. Their value for every size of the training set can be determined by solving the following optimisation problem [65]:

$$f_\beta = \underset{\{q_k, m_k, V_k, \hat{q}_k, \hat{m}_k, \hat{V}_k, b\}_{k=+,-}}{\text{extr}} \left[\sum_{k=+,-} -\frac{1}{2} \left(\hat{q}_k V_k - q_k \hat{V}_k \right) + m_k \hat{m}_k + \lim_{p \rightarrow \infty} \frac{1}{p} \Psi_s + \alpha \gamma \Psi_e \right]. \quad (\text{C.2})$$

where the entropic potential Ψ_s can be expressed as a function of the means $\boldsymbol{\mu}_\pm \in \mathbb{R}^p$ and covariances $\Sigma_\pm \in \mathbb{R}^{p \times p}$ of the hidden-layer activations of the random features model, while the energetic potential Ψ_e depends on the specific choice of the loss function $\ell(\cdot)$.

Solving the optimization problem in eq. (C.2), leads to a set of coupled saddle-point equations for the overlap parameters and the bias term. This set of equations is nothing but a special case of the equations already derived in [65], that is high-dimensional classification of a mixture of two Gaussians with random features, except for the typo in the self-consistency equation of the bias term

$$b = \left(\sum_{k=\pm} \frac{\rho_k}{V_k} \right)^{-1} \sum_{k=\pm} \rho_k \mathbb{E}_\xi [\eta_k - m_k], \quad (\text{C.3})$$

with η_k being the extremizer

$$\eta_k = \underset{\lambda}{\operatorname{argmin}} \left[\frac{(\lambda - \sqrt{q_k} \xi - m_k - b)^2}{2V_+} + \ell(y_k, \lambda) \right]. \quad (\text{C.4})$$

and $\ell(\cdot)$ being any convex loss function. Analogously to the more general setting of [65], the Gaussian Equivalence Theorem allows to express the entropic potential Ψ_s as a function of the means $\boldsymbol{\mu}_k \in \mathbb{R}^p$ and covariances $\Sigma_k \in \mathbb{R}^{p \times p}$ of the random features

$$\begin{aligned} \Psi_s = & \lim_{p \rightarrow \infty} \frac{1}{p} (\hat{q}_+ \boldsymbol{\mu}_+ + \hat{q}_- \boldsymbol{\mu}_-)^t \left(\lambda \mathbb{I}_p + \hat{V}_+ \Sigma_+ + \hat{V}_- \Sigma_- \right)^{-1} (\hat{q}_+ \boldsymbol{\mu}_+ + \hat{q}_- \boldsymbol{\mu}_-) + \\ & + \lim_{p \rightarrow \infty} \frac{1}{p} \operatorname{Tr} \left((\hat{q}_+ \Sigma_+ + \hat{q}_- \Sigma_-) \left(\lambda \mathbb{I}_p + \hat{V}_+ \Sigma_+ + \hat{V}_- \Sigma_- \right)^{-1} \right); \end{aligned} \quad (\text{C.5})$$

while the energetic potential Ψ_e depends on the specific choice of the loss function $\ell(\cdot)$

$$\Psi_e = -\frac{1}{2} \mathbb{E}_\xi \left[\sum_{k=\pm} \rho_k \frac{(\eta_k - \sqrt{q_k} \xi - m_k - b)^2}{2V_k} + \ell(y_k, \eta_k) \right]. \quad (\text{C.6})$$

As discussed in section 4.1, the Gaussian Equivalence Theorem breaks in the quadratic sample regime if the data are sampled from the spiked Wishart model. Interestingly, this is not the case for the Hidden Manifold model. Indeed, as shown in fig. C.1, we still get a perfect match between the Gaussian theory and the numerical simulations even in the quadratic sample regime. The theoretical prediction can be easily derived by rescaling the free-energy associated to the Hidden Manifold model as in [67] by a factor $1/d^2$. This is the same trick already proposed in [75] for teacher-student settings and displayed in the middle panel of fig. C.1.

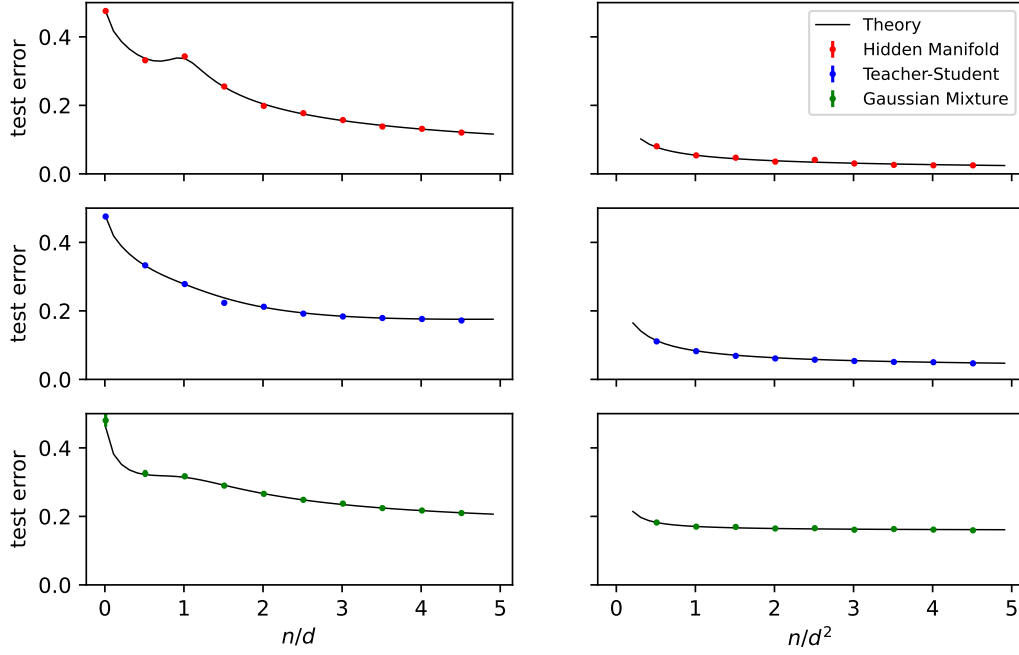


Figure C.1: **Linear and quadratic sample regimes for different synthetic data models.** (*Right*) Generalization error of the hidden manifold model (top), the teacher-student setup (center) and a mixture of two Gaussian as a function of the ratio of the number of samples and the input dimension. (*Left*) Same except that the number of samples scales with the square of the input dimension. The solid black line corresponds to the replica theory prediction while the colored dots display the outcome of the numerical simulations averaged over 10 different seeds. In all panels, $d = 1000$ and $d = 20$ for linear and quadratic sample regimes respectively, $\lambda = 0.01$ for both the teacher-student setup and the hidden manifold model while $\lambda = 0.1$ for Gaussian mixtures. In the Gaussian mixture case, $\mu_{\pm} = (\pm 1, 0, \dots, 0) \in \mathbb{R}^d$ while the covariance matrices are both isotropic and, in particular, both equal to the identity matrix: $\Sigma_{\pm} = \mathbb{I}$.